

---

---

**Optics and photonics — Interferometric  
measurement of optical elements and  
optical systems —**

**Part 3:  
Calibration and validation of  
interferometric test equipment and  
measurements**

*Optique et photonique — Mesurage interférométrique de composants  
et systèmes optiques —*

*Partie 3: Étalonnage et validation des équipements d'essai  
interférométrique*



Reference number  
ISO/TR 14999-3:2005(E)

© ISO 2005

**PDF disclaimer**

This PDF file may contain embedded typefaces. In accordance with Adobe's licensing policy, this file may be printed or viewed but shall not be edited unless the typefaces which are embedded are licensed to and installed on the computer performing the editing. In downloading this file, parties accept therein the responsibility of not infringing Adobe's licensing policy. The ISO Central Secretariat accepts no liability in this area.

Adobe is a trademark of Adobe Systems Incorporated.

Details of the software products used to create this PDF file can be found in the General Info relative to the file; the PDF-creation parameters were optimized for printing. Every care has been taken to ensure that the file is suitable for use by ISO member bodies. In the unlikely event that a problem relating to it is found, please inform the Central Secretariat at the address given below.

© ISO 2005

All rights reserved. Unless otherwise specified, no part of this publication may be reproduced or utilized in any form or by any means, electronic or mechanical, including photocopying and microfilm, without permission in writing from either ISO at the address below or ISO's member body in the country of the requester.

ISO copyright office  
Case postale 56 • CH-1211 Geneva 20  
Tel. + 41 22 749 01 11  
Fax + 41 22 749 09 47  
E-mail [copyright@iso.org](mailto:copyright@iso.org)  
Web [www.iso.org](http://www.iso.org)

Published in Switzerland

**Contents**

Page

<b>Foreword</b> .....	<b>iv</b>
<b>Introduction</b> .....	<b>v</b>
<b>1 Scope</b> .....	<b>1</b>
<b>2 Terms and definitions</b> .....	<b>1</b>
<b>3 Systematical investigation of test equipment, test set-up and test environment for sources of errors</b> .....	<b>2</b>
<b>3.1 General</b> .....	<b>2</b>
<b>3.2 Sources of uncertainty</b> .....	<b>2</b>
<b>3.3 Combination of uncertainties</b> .....	<b>3</b>
<b>4 Separation of errors into rotationally symmetric and non-rotationally symmetric terms</b> .....	<b>4</b>
<b>4.1 General</b> .....	<b>4</b>
<b>4.2 Principle</b> .....	<b>4</b>
<b>4.3 Apparatus</b> .....	<b>6</b>
<b>4.4 Procedure</b> .....	<b>6</b>
<b>5 Measurement relying on the quality of a physical reference surface</b> .....	<b>6</b>
<b>5.1 Planes</b> .....	<b>6</b>
<b>5.2 Spheres</b> .....	<b>9</b>
<b>5.3 Aspheres</b> .....	<b>12</b>
<b>5.4 Homogeneity testing</b> .....	<b>24</b>
<b>5.5 Optical systems in transmission</b> .....	<b>25</b>
<b>6 Optical test procedures for achieving absolute calibration</b> .....	<b>28</b>
<b>6.1 General</b> .....	<b>28</b>
<b>6.2 Flats</b> .....	<b>29</b>
<b>6.3 Spherical surfaces</b> .....	<b>35</b>
<b>6.4 Cylindrical surfaces</b> .....	<b>41</b>
<b>6.5 Windows in transmission</b> .....	<b>42</b>
<b>Bibliography</b> .....	<b>44</b>

## Foreword

ISO (the International Organization for Standardization) is a worldwide federation of national standards bodies (ISO member bodies). The work of preparing International Standards is normally carried out through ISO technical committees. Each member body interested in a subject for which a technical committee has been established has the right to be represented on that committee. International organizations, governmental and non-governmental, in liaison with ISO, also take part in the work. ISO collaborates closely with the International Electrotechnical Commission (IEC) on all matters of electrotechnical standardization.

International Standards are drafted in accordance with the rules given in the ISO/IEC Directives, Part 2.

The main task of technical committees is to prepare International Standards. Draft International Standards adopted by the technical committees are circulated to the member bodies for voting. Publication as an International Standard requires approval by at least 75 % of the member bodies casting a vote.

In exceptional circumstances, when a technical committee has collected data of a different kind from that which is normally published as an International Standard ("state of the art", for example), it may decide by a simple majority vote of its participating members to publish a Technical Report. A Technical Report is entirely informative in nature and does not have to be reviewed until the data it provides are considered to be no longer valid or useful.

Attention is drawn to the possibility that some of the elements of this document may be the subject of patent rights. ISO shall not be held responsible for identifying any or all such patent rights.

ISO/TR 14999-3 was prepared by Technical Committee ISO/TC 172, *Optics and photonics*, Subcommittee SC 1, *Fundamental standards*.

ISO 14999 consists of the following parts, under the general title *Optics and photonics — Interferometric measurement of optical elements and optical systems*:

- *Part 1: Terms, definitions and fundamental relationships* (Technical Report)
- *Part 2: Measurement and evaluation techniques* (Technical Report)
- *Part 3: Calibration and validation of interferometric test equipment and measurements* (Technical Report)
- *Part 4: Interpretation and evaluation of tolerances specified in ISO 10110*

## Introduction

A series of International Standards on *Indications in technical drawings for the representation of optical elements and optical systems* has been prepared by ISO/TC 172/SC 1, and published as ISO 10110 under the title *Optics and photonics — Preparation of drawings for optical elements and systems*. When drafting this standards series and especially its Part 5, *Surface form tolerances*, and Part 14, *Wavefront deformation tolerances*, it became evident to the experts involved that additional complementary documentation is required to describe how the necessary information on the conformance of the fabricated parts with the stated tolerances can be demonstrated. Therefore, the responsible ISO Committee ISO/TC 172/SC 1 decided to prepare an ISO Technical Report on *Interferometric measurement of optical wavefronts and surface form of optical elements*.

When discussing the topics which had to be included or excluded into such a Technical Report, it was envisaged that it might be the first time, where an ISO Technical Report or Standard is prepared which deals with wave-optics, i.e. that is based more in the field of physical optics than in the field of geometrical optics. As a consequence only fewer references than usual were available, which made the task more difficult.

Envisaging the situation, that the topic of interferometry has so far been left blank in ISO, it was the natural wish to now be as comprehensive as possible. Therefore there was discussion, whether important techniques such as interference microscopy (for characterizing the micro-roughness of optical parts), shearing interferometry (e.g. for characterizing corrected optical systems), multiple-beam interferometry, coherence sensing techniques or phase conjugation techniques should be included or not. Other techniques, which are related to the classical two-beam interferometry, like holographic interferometry, Moiré techniques and profilometry were also mentioned as well as Fourier transform spectroscopy or the polarization techniques, which are mainly for microscopic interferometry.

In order to complement ISO 10110, the guideline adopted was to include what nowadays are common techniques used for the purpose of characterizing the quality of optical parts. Decision was made to complete a first Technical Report, and to then update it by supplementing new parts, as required. It is very likely that more material will be added in the near future as more stringent tolerances (two orders of magnitude) for optical parts and optical systems become mandatory, when dealing with optics for the EUV range (wavelength range 6 nm to 13 nm) for microlithography. Also, testing optics with EUV radiation (the same wavelength as they are later used, e.g. at-wavelength testing) can be a new challenge, and is not covered by any current standards.

This part of ISO 14999 should cover the need for qualifying optical parts and complete systems regarding the wavefront error produced by them. Such errors have a distribution over the spatial frequency scale; in this part of ISO 14999 only the low- and mid-frequency parts of this error-spectrum are covered, not the very high end of the spectrum. These high-frequency errors can be measured only by microscopy, measurement of the scattered light or by non-optical probing of the surface.

A similar statement can be made regarding the wavelength range of the radiation used for testing. ISO 14999 considers test methods with visible light as the typical case. In some cases, infrared radiation from CO<sub>2</sub>-lasers in the range of 10,6 µm is used for testing rough surfaces after grinding or ultraviolet radiation from excimer-lasers in the range of 193 nm or 248 nm is used for at-wavelength testing of microlithography optics. However, these are still rare cases, which are included in standards, that will not be dealt with in detail. The wavelength range outside these borders is not covered.

.....

# Optics and photonics — Interferometric measurement of optical elements and optical systems —

## Part 3: Calibration and validation of interferometric test equipment and measurements

### 1 Scope

This part of ISO 14999 discusses sources of error and the separation of errors into symmetric and non-symmetric parts. It also describes the reliance of measurements on the quality of a physical reference surface and the development of test procedures capable of achieving absolute calibration.

### 2 Terms and definitions

For the purposes of this document, the following terms and definitions apply.

#### 2.1

##### **perfect shape**

mathematically represented figure of the optical surface

#### 2.2

##### **surface error**

deviation from the perfect shape of the surface under test, including the influence of gravity and support

#### 2.3

##### **wavefront error**

error of the interferometric wavefront corresponding to the surface error

#### 2.4

##### **absolute test**

method, which gives the wavefront error of the test piece with respect to a perfect shape, not to a bodily reference

#### 2.5

##### **quasi-absolute test**

method, which gives the wavefront error, limited to special error types, of the test piece with respect to a perfect shape, not a bodily reference

### 3 Systematical investigation of test equipment, test set-up and test environment for sources of errors

#### 3.1 General

The objective of a measurement is to determine the value of the measurand, that is the specific quantity subject to measurement. In the general context of testing and calibration laboratories, the measurand may cover many different quantities, but in the context of this Technical Report it is an optical parameter, such as wavefront shape, associated with optical elements or optical systems. A measurement begins with an appropriate specification of the measurand, the generic method of measurement and the specific detailed measurement procedure.

No measurement is perfect and the imperfections give rise to error of measurement in the result. Consequently, the result of a measurement can only be an approximation to the value of the measurand and it is only complete when accompanied by a statement of the uncertainty of that approximation. Because of measurement uncertainty the *true value* can never be known.

Uncertainty of measurement comprises many components. Some may be evaluated from the statistical distribution of the results of a series of measurements and can be characterized by experimental standard deviations. The other components are based on experience or other information and are evaluated from assumed probability distributions. They are also characterized by (equivalent) standard deviations.

Random errors arise from random variations of the observations, due to random effects from various sources affecting measurements taken under nominally the same conditions. These produce a scatter around the mean value of a series of measurements. They cannot be eliminated but the uncertainty due to their effect can be reduced by increasing the number of observations and applying statistical analysis.

Systematic errors arise from systematic effects, that is an effect on the measurement result arising from a quantity that is not included in the measurement specification of the measurand but influences the result. These remain unchanged when the measurement is repeated under the same conditions. Examples might be drifts during measurements or since the last calibration of a measuring instrument, zero errors in scales, errors in assumed expansion coefficients, etc. Their effect is to introduce a displacement, or bias, between the value of the measurand and the experimentally determined mean value. They cannot be eliminated but may be reduced by making corrections for the *known extent* of an error due to a recognized systematic effect.

The total uncertainty of measurement is a combination of all identified component uncertainties. Careful consideration of each measurement involved in the test or calibration is required to identify and list all the factors that contribute to the overall uncertainty. This is a very important step that requires a good understanding of the measurement equipment, the process of the test or calibration and the influence of the environment.

Having identified the component uncertainties, the next step is to quantify them by appropriate means. An initial approximate quantification can be valuable in identifying components that are negligible, less than one fifth the largest component, and not worthy of more rigorous evaluation. Uncertainties from random sources, classified as *Type A*, may be quantified by calculation of the standard deviation of repeated measurements. Uncertainties from systematic sources, classified as *Type B*, require an exercise of judgement by the metrologist, using all relevant information on their possible variability, to evaluate effective standard deviations.

Subsequent calculations are made simpler if, wherever possible, all components are expressed in the same way, e.g. as a proportion, or in the same units as used for the reported result.

#### 3.2 Sources of uncertainty

There are many possible sources of uncertainty, which will depend on the technical discipline involved. However, the following general points will apply to many areas of optical testing and calibration:

- incomplete definition of the test; the requirement may not be clearly described in sufficient detail;



- imperfect realization of the test procedure; even when the test conditions are clearly defined, it may not be possible to produce the theoretical conditions in practice due to imperfections in the systems used;
- personal bias in the reading of analogue instruments and scales;
- instrument resolution or discrimination threshold, errors in scales;
- values attributed to measurement standards and reference artifacts;
- changes in characteristics or performance of a measuring instrument or reference artifact since the last calibration;
- approximations and assumptions incorporated in the measurement method and procedure;
- random effects in repeated measurements.

These sources are not necessarily independent and, in addition, unrecognized systematic effects may exist that cannot be taken into account but contribute to the error. It is for this reason that interlaboratory comparisons, measurement audits and internal cross-checking of results by different means are undertaken.

NOTE Sources of uncertainty specific to the interferometric evaluation of optical elements and optical devices will be included as they become identified.

### 3.3 Combination of uncertainties

Once the uncertainty contributions associated with a measurement process have been identified and quantified, it is necessary to combine them in some manner in order to provide a single value of uncertainty that can be associated with the measurement result.

There is no *correct way* of combining uncertainties. The ISO *Guide to the expression of uncertainty of measurement*, known as the *GUM*, is the accepted method for most laboratories and accreditation bodies, but it is only a guide, a set of conventions.

By using a predetermined set of conventions, such as presented in *the GUM*, laboratories and their clients are able to compare results from different sources in a meaningful manner. This is also true of uncertainties passed down from national standards institutions and secondary standards laboratories.

The combination process may be summarized as follows:

- a) individual uncertainties are evaluated by the appropriate method and each is expressed as a standard deviation, referred to as a standard uncertainty;
- b) the individual standard uncertainties are combined, by the root of the sum of squares method, to produce an overall value of uncertainty, known as the combined standard uncertainty;
- c) an expanded uncertainty is obtained by multiplying the combined standard uncertainty by a coverage factor,  $k$ . The choice of factor is based on the level of confidence required. A value of  $k = 2$  is usually chosen, corresponding to a confidence level of approximately 95 %.

There are some exceptions to this general guidance. Reference should be made to the *GUM* for further information.

## 4 Separation of errors into rotationally symmetric and non-rotationally symmetric terms

### 4.1 General

The separation of errors into rotationally symmetric and non-rotationally symmetric terms is a powerful tool in practice as it makes possible the collection of a lot of information by simple means. It should be used with care because it does not determine the rotationally symmetric errors of the test piece. Nevertheless in practice very often rotationally symmetric error terms do not influence the results as much as non-rotationally terms does.

Subclauses 4.2 to 4.4 establish the procedure to separate measured wavefront errors of optical components into rotationally symmetric and non-rotationally symmetric terms to determine the non-rotationally symmetric surface errors of the test piece in an absolute sense.

The method is applicable to all optical surfaces with rotationally symmetric shape, including flats, spheres, and aspheres. It is also applicable to test optical components or systems in transmission.

The method is not applicable to optical surfaces without rotationally symmetric shape, e.g. off-axis aspheres. It is not applicable to determine the rotationally symmetric errors of the test piece in an absolute sense.

### 4.2 Principle

Two beam interferometers used for wavefront testing always measure the difference between the wavefront errors of the test piece and the wavefront errors of the interferometer which can not be separated by a single measurement. The interferometer errors include for example errors of the reference surface, errors of the transmission spheres or compensation optics. To determine the errors of the test piece, reference standards or so-called absolute tests shall be used. But there are a few well known procedures available for practical usage. The best known of the absolute tests, which do not need any auxiliary optics, is the three-position test <sup>[1]</sup> for spheres with accessible focus. But there are no easy and cheap solutions for absolute tests of flats, convex spheres, aspheres or optical components in transmission.

A quasi-absolute test of the non-rotationally symmetric wavefront errors can be based on the measurements of the test piece under different angles of rotation ( $\theta$ , Figure 1) and on the error

$$P(r, \theta) = P_R(r) + P_{NR}(r, \theta) \quad (1)$$

where

$P_R(r)$  is the rotationally symmetric term;

$P_{NR}(r, \theta)$  is the non-rotationally symmetric term.

If the interferometer error is also split into a rotationally symmetric term  $T_R(r)$  and a non-rotationally symmetric term  $T_{NR}(r, \theta)$ , the measured wavefront error can be expressed as

$$W = T_R + P_R + P_{NR} \quad (2)$$

as sum of all the rotationally and non-rotationally symmetric terms.

It can be shown <sup>[2]</sup> <sup>[3]</sup> <sup>[4]</sup>, that rotating a wavefront to  $N$  (where  $N = 2, 3, \dots$ ) equally spaced positions at  $2\pi / N$  intervals and then averaging the data reduces to zero all non-rotationally symmetric terms except those of order  $kN\theta$ , where  $k = 1, 2, \dots$

This can be used to separate the non-rotationally symmetric errors of the test piece by measuring  $N$  rotational positions and averaging the results. Explicitly, the procedure can be written as a series of measurements  $W_i$ ,  $i = 1, \dots, N$ :

$$W_1 = T_R + T_{NR} + P_R + P_{NR}^1 \quad (3)$$

$$W_2 = T_R + T_{NR} + P_R + P_{NR}^2$$

etc.

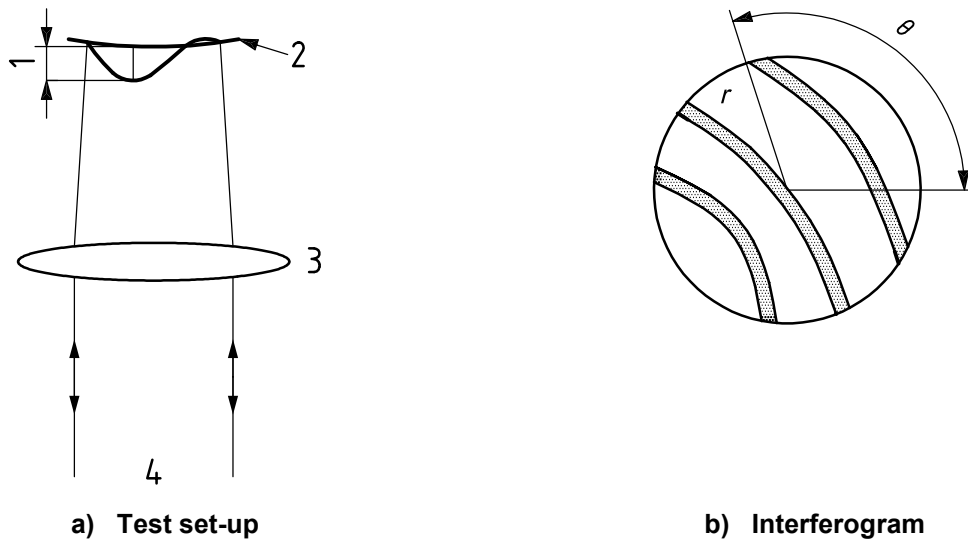
By averaging these measurements to reduce the non-rotationally symmetric terms of the test part to zero except those of order  $kN\theta$ , the following is obtained:

$$W_A = T_R + T_{NR} + P_R + P_{NR}^{kN\theta} \quad (4)$$

Thus,

$$W_1 - W_A = P_{NR} - P_{NR}^{kN\theta} \quad (5)$$

which may be subtracted from any of the measurements  $W_i$ , appropriately orientated, to give the non-rotationally symmetric terms of the test piece except those of order  $kN\theta$ .



**Key**

- 1 surface error  $S(r, \theta)$
- 2 perfect shape
- 3 lens
- 4 plane wave from interferometer

The relation between the surface error  $S$  and the measured wavefront error  $P$  is  $P = 2 S$ .

**Figure 1 — Schematic diagram of an interferometric test set-up for testing a convex surface in reflection**

If the data of the single measurements are rotated back before averaging, then the following are obtained:

$$W_B = T_R + T_{NR}^{kN\theta} + P_R + P_{NR} \quad (6)$$

and

$$W_1 - W_B = T_{NR} - T_{NR}^{kN\theta} \quad (7)$$

which is the non-rotationally symmetric term of the interferometer errors except those of order  $kN\theta$ .

### 4.3 Apparatus

The minimum test apparatus required to perform the specified test procedure is listed below.

**4.3.1 Interferometer**, with digital data readout.

**4.3.2 Qualified test set-up**.

**4.3.3 Rotation stage**, for the test piece.

**4.3.4 Evaluation software**, with the ability to average and difference (rotate) wave front data.

### 4.4 Procedure

The test piece shall be measured in  $N \geq 4$  equally spaced rotational positions. Proceed as follows.

- a) Measure the test piece in the first rotational position and store the wavefront data, piston and tilt may be subtracted.
- b) Rotate the test piece about  $2\pi / N$ ,  $N \geq 4$ , and repeat the measurement. Store the wavefront data.
- c) Repeat step b) measuring  $N$  rotational positions in total.
- d) Calculate the average of the  $N$  measurements and store the averaged wavefront data.
- e) Subtract the result from the measurement obtained in a) and store the final result.

## 5 Measurement relying on the quality of a physical reference surface

### 5.1 Planes

#### 5.1.1 General

In this case, there are

- a) a plane master as reference mirror, and
- b) a roughly plane sample, or optical system emitting a plane wavefront, to be measured.

Incidence beams are propagated as plane wavefronts under quasi normal incidence onto the master and the sample. Both surfaces reflect the wavefront modified by their surface defaults. The interferogram is generated by the distorted emergent wavefronts and contains the required information.

As described, adjustment of the relative position of the master surface and the sample allow the user to modify the interference pattern.

- By tilting, the inter-fringe spacing, i.e. the sensitivity of the measurement, can be enhanced or reduced (interval between two fringes represents a mechanical gradient of  $\lambda/4$  on the sample).
- By translation (translation parallel to the optical axis), one can enhance a small and local default, by placing a fringe ramp on it.

Because the beams reflect only once from the reference mirror and from the measured object, the interference pattern cannot emphasize a small defect. The user should note that the Michelson interferometer is not able to provide information about surface errors to much better than  $\lambda/10$ .

## 5.1.2 Measurement relying on a plane master

### 5.1.2.1 Perfect plane master

For some applications, the plane master may be considered perfect, or assumed to be of a quality at least ten times better than the sample.

The user may then consider the interferogram as generated by a perfect wavefront (returning from the master) and an aberrated one, coming back from the sample. The aberrations of this wavefront, made visual by the interferogram, can qualify the sample.

### 5.1.2.2 Imperfect plane master

In many applications, the plane master cannot be considered perfect in comparison to the sample. The user shall then consider the interferogram as being the summation of the defaults of both surfaces.

In order to determine amplitudes and positions of the defaults on the sample and on the master, the user can compare to the first measurement one or more measurements generated by

- a translation of the master (with respect to the sample) in its surface plane;
- a rotation of the master (with respect to the sample) around the optical axis.

The user

- can create more than one translation, in more than one direction;
- can generate more than one rotation; and
- can combine translation(s) and rotation(s).

See Figures 2 and 3.

By comparing the different interference patterns issuing from the different relative positions, the user may determine the localization and amplitude of the defects (remembering that an interferogram represents the algebraic addition of aberrations).

### 5.1.2.3 Determination of plane master quality

The plane master to be used as a reference shall be qualified. This may be made with a second plane mirror (or better with two additional plane mirrors) of the same quality.

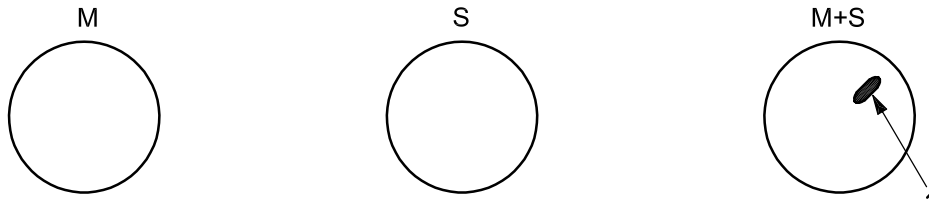
The quality determination is achieved using the procedure described in 5.1.2.2, by carrying out measurements with different combinations.

**EXAMPLE** With three-plane mirrors available, the user tests No. 1 against No. 2, No. 1 against No. 3, No. 2 against No. 3, and extracts the mapping of the objects No. 1, No. 2, No. 3. This is referred to as the “three-planes method” (see 6.2).

## 5.1.3 Calibration certificate

Commercially made interferometers and ancillary reference plane surfaces should come with fully authenticated calibration documents.

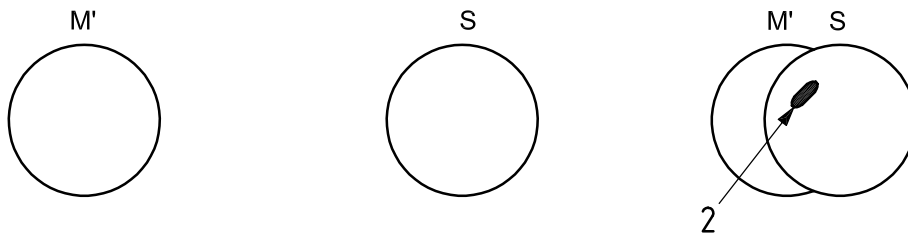
A calibration certificate for a reference surface should indicate the departure from flatness, and should also contain detailed mapping of the position and size of defects.



**Key**

- 1 information 1
- M master in initial position
- S sample in initial position
- M+S initial interference pattern

**a) Observations at initial positions**



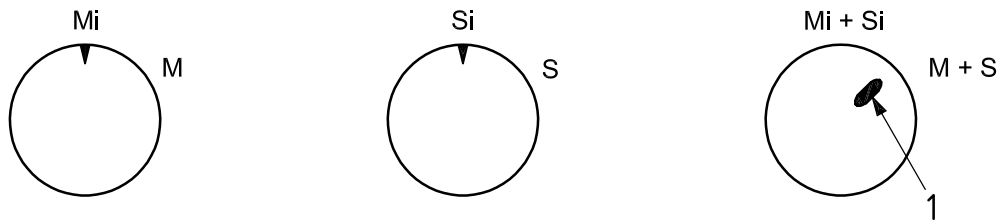
**Key**

- 2 information 2
- M' master after translation
- S sample
- M', S second interference pattern

**b) Observations after a translation of master**

The master and sample can be individually observed by the introduction of an opaque screen in the interferometer arms. Translation vectors can be carried by the master and/or the sample. Direction and length of the vectors are chosen by the user. The user can execute one or more translations. Interference patterns are generated by the algebraic summation of the defects present on both surfaces. The interference pattern gives information about both surfaces. The user can mix effects from translation(s) and rotation(s); see Figure 3.

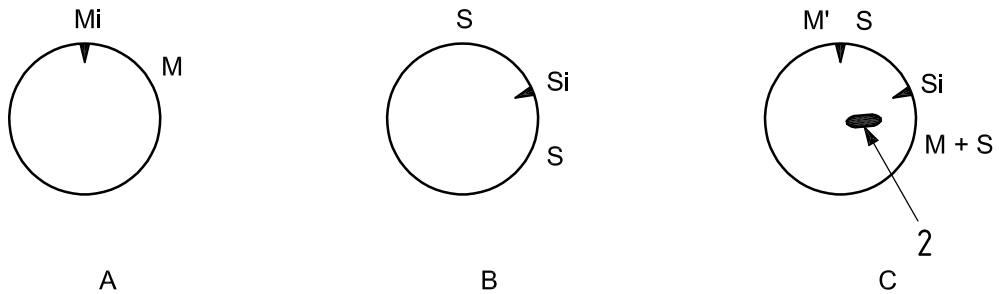
**Figure 2 — Examples of interference patterns and translation effects**



**Key**

- 1 information 1
- M master in initial position
- Mi master index
- S sample in initial position
- Si sample index
- M+S, Mi+Si initial interference pattern

**a) Observations at initial positions**



**Key**

- 2 information 2
- A master
- B sample after rotation
- C second interference pattern

**b) Observations after a rotation of sample**

The master and sample can be individually observed by the introduction of an opaque screen in the interferometer arms. Rotations can be carried out on either the master and/or the sample. Rotation angles are chosen by the user. The user can execute one or more rotations. Interference patterns are generated by the algebraic summation of defects present on both surfaces. The interference pattern gives information about both surfaces. The user can mix effects from rotation(s) and translation(s); see Figure 2.

**Figure 3 — Examples of interference patterns and rotation effects**

**5.2 Spheres**

**5.2.1 General**

The optical quality of concave and convex wavefronts can be analysed relative to a physical spherical surface of known (calibrated) quality, with the usual reservations in relation to the source coherence.

Both a spherical wavefront and spherical reference surface have a centre of curvature.

To achieve the required optical interference pattern, both centres shall be located close to each other. The user has to modify the interferometer adjustment and/or components in both optical arms, in order to superimpose the centres of curvature as well as possible.

### 5.2.2 Measurement relying on a perfect master

Each misadjustment of the centres generates an interference pattern, related to the optical path differences between two spherical wavefronts coming back to the observer or measurement devices.

In order to adjust the instrument, imagine the following interference pattern generated by a dipole.

- a) Both centres are on the optical axis, one translated behind the other one: the interferogram is a collection of concentric rings.
- b) Both centres are on the same plane, perpendicular to the optical axis: the interferogram is the Young interference pattern (a collection of linear fringes).
- c) At least one centre is off the optical axis and not in the same plane as the other centre: the interferogram is either elliptical or hyperbolic.

The adjustment of the interferometer controls should be made in order to generate concentric rings noting:

- the inter-fringe spacing increases when the two centres coincide;
- the zero order is reached when the considered centres are superposed;
- the residual interference pattern corresponds to the defects of the analysed sample.

### 5.2.3 Qualification of the master

A “three bowls method” allows the user to determine the quality of a spherical master, as does the “three-planes method” for plane masters (see also 6.3).

An optical workshop can generate matching pairs of concave and convex spherical master surfaces, of the same radius value, by polishing them together.

The qualification procedure is the same as for plane masters.

### 5.2.4 Alternative method

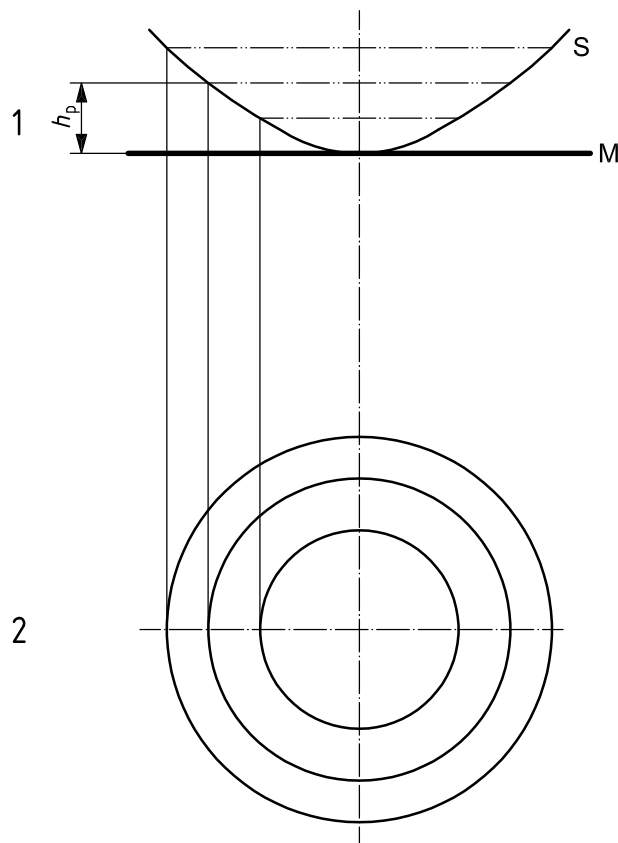
This method is valid for spheres of long radius (radius of curvature in excess of several metres).

The reference master can be a plane mirror and the observed interference pattern is a distribution of concentric rings when alignment is well realized.

The user can check the regularity of the surface curvature by checking the spacing of the fringes.

The interference pattern is directly linked to the relative positions of the flat mirror and the sphere. The user can, therefore, imagine how the different possible relative positions generate interference patterns (see Figure 4). Fringes are visible when  $h_0 = p\lambda/2$ . In the case of one point contact (as shown in Figure 4), the radius of fringes is  $R_N = k\sqrt{N} + R_0$ , with  $R_N$ , radius of the  $N$ th fringe,  $k$ , fixed coefficient and  $R_0$ , interference state at the contact point.





**Key**

- 1 images of the plane mirror and of the spherical mirror
- 2 images of the interference pattern

M master  
 S spherical mirror  
 $h_p$  sagitta

**a) Observation of Newton's rings (parallel axes)**

	Tilted axes	Parallel axes	Tilted axes
No contact			
1-point contact			
Section			

**b) Table indicating position of sphere relative to that of flat mirror**

**Figure 4 — Calibration of a long radius sphere**

## 5.3 Aspheres

### 5.3.1 Types of aspheres

#### 5.3.1.1 General

Since the test of general aspheres lacks the possibility of self-consistent absolute measurements which can be performed for plane and spherical surfaces, it is necessary to distinguish the aspheres according to the test complexity they provoke.

Since all interferometric test methods rely on the comparison of two common wavefronts, i.e. the superposition of the wavefront generated by the aspherical surface and a reference wavefront or the superposition of two displaced copies of the aspherical wavefront, the complexity of the test situation is governed by the difficulties in establishing a suitable reference wavefront.

In interferometry, in general, plane or spherical wavefronts are dealt with which can easily be transformed into one another by the use of diffraction-limited optics, on the one hand, and on the other which can be calibrated by absolute measuring methods relying only on the combination of suitably chosen relative measurements, i.e. measurements where the test piece is adjusted in different arrangements. In this sense, the plane and spherical wavefronts and simple optical elements like plane and spherical surfaces play a key role due to their imminent calibration potential.

A further general aspect is the necessity to use interferometric methods to generate low spatial frequency interferograms. There are at least two fundamental reasons for this limitation. The first is connected with the sampling theorem and the ability of detecting devices to store a unique representation of wavefront data and the second has to do with the inevitable measuring errors if large deviations are present within the interferogram. If the gradient of the deviations becomes large or if the phase difference between test wavefront and reference becomes too large, then all alignment errors and inaccuracies in the lateral position in the interferogram translate into large measuring errors.

For this reason, it is necessary to discern between the following types of aspheres where the test complexity increases in the given order:

- stigmatic;
- slow;
- steep aspheres.

#### 5.3.1.2 Stigmatic aspheres

Stigmatic aspheres are those which transform one spherical wavefront into another having a different radius of curvature. The case of the transformation of plane into spherical wavefronts is also covered by this definition.

Stigmatic aspheres, as for example conical surfaces (paraboloids, ellipsoids and hyperboloids), can be tested in interferometers of the Twyman-Green type or similar arrangements since they transform spherical wavefronts into spherical wavefronts or plane into spherical and vice versa. In nearly all cases, it is possible to give a combination of some high-aperture optics which enables the comparison of the wavefront generated by the aspheric with a plane or a simple spherical wavefront [5]. In most interferometers, it is preferable to use plane reference wavefronts since the beam splitter and the recombiner of the beams could otherwise introduce systematic errors into the measurement.

#### 5.3.1.3 Slow aspheres

Slow aspheres are those surfaces that either deviate only weakly from a plane or spherical surface of suitable radius of curvature. Therefore it is possible to test them with proof-glass-related methods, e.g. within a Fizeau interferometer with suitable illumination optics, i.e. optics which generates an illuminating wavefront having the curvature of the reference surface.

### 5.3.1.4 Steep aspheres

This is the most complex case requiring extraordinary skill of the experimenter and the technical means to produce suitable reference waves. In this connection, it is possible to think of compensating devices as null optics made of simple lens elements or even whole optical systems generating the conjugate of the ideal aspherical wavefront at least in the test configuration or in the most general case the use of computer-generated holograms or diffracting optical elements which provide both the reference wave and its conjugate to enable the most general use as reference masters for aspherical testing.

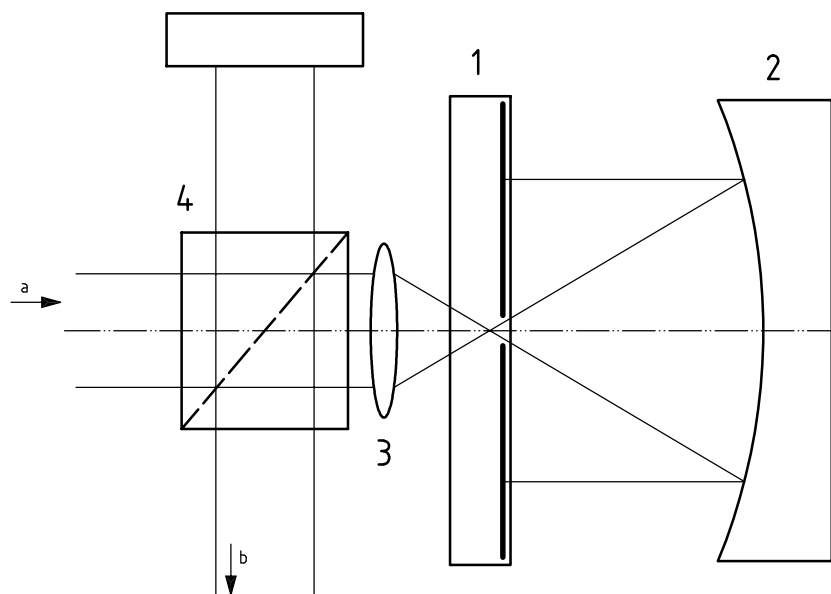
### 5.3.2 Test methods

#### 5.3.2.1 Test methods for stigmatic aspheres

Stigmatic aspheres can be tested in Twyman-Green or similar arrangements. Some auxiliary optics have to be used in order to guarantee plane wave input/output to the interferometer.

Here only two examples will be described in more detail to give a general impression of the test philosophy.

Figure 5 shows the arrangement for the test of paraboloids. Figure 6 gives the test arrangement for ellipsoidal mirrors.



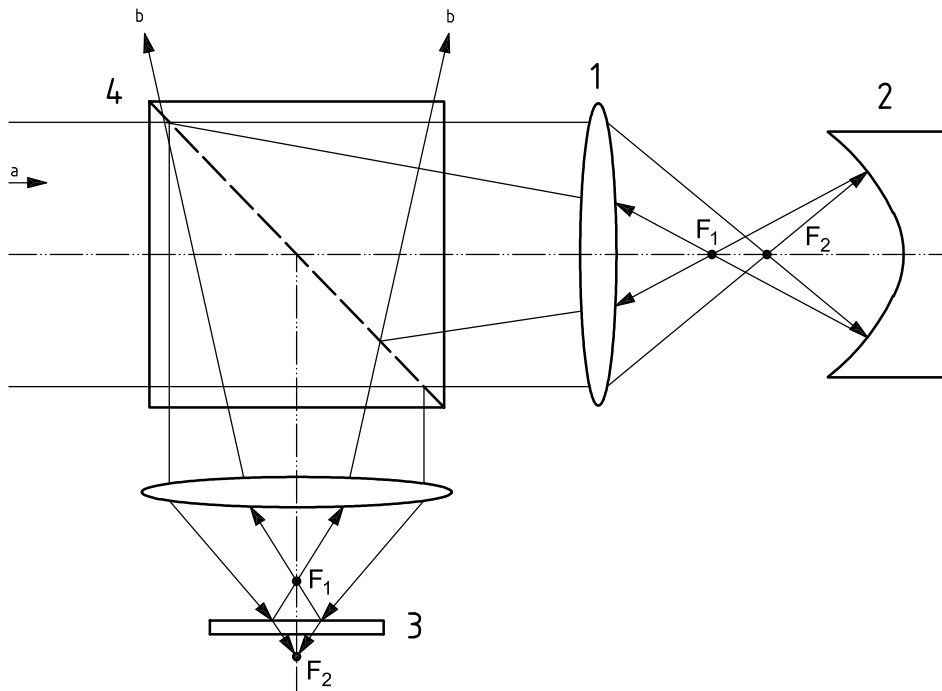
#### Key

- 1 plane mirror
- 2 paraboloid
- 3 beam-shaping optics
- 4 polarizing beam splitter

a From laser.

b To detector.

Figure 5 — Paraboloid test



**Key**

- 1 beam-shaping optics
- 2 ellipsoid
- 3 plane reference mirror
- 4 beam splitter

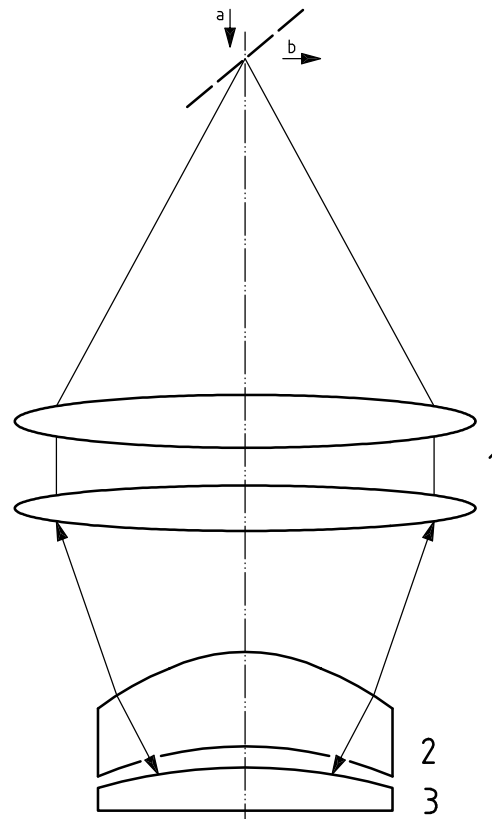
- $F_1$  focal point of the emerging wave
- $F_2$  focal point of the incident wave

- a From laser.
- b To detector.

**Figure 6 — Test for an ellipsoidal mirror**

**5.3.2.2 Proof-glass or Fizeau-type tests**

Slow or weak aspheres can be tested by combining the aspherical surface with a spherical or, in some cases, plane proof glass of matching curvature. Matching means that the resulting Fizeau interferometer produces a low-frequency interferogram. The maximum of possible aspheric excursion from a matching sphere is determined by the sampling theorem and the limitations of systematic evaluation errors. In every case, a careful systematic error analysis is necessary to find out which is the best illuminating wavefront. A first approach is evidently the choice of an illuminating wavefront matching the reference surface. Figure 7 shows a typical example for a slow convex aspheric. A first guess for the applicability of this test procedure is deviations of the order of a few  $\mu\text{m}$  from a best-fitting sphere.

**Key**

- 1 beam-shaping optics
- 2 spherical reference
- 3 aspheric

- a From laser.
- b To detector.

**Figure 7 — Fizeau test of a convex aspheric with the help of a spherical proof glass**

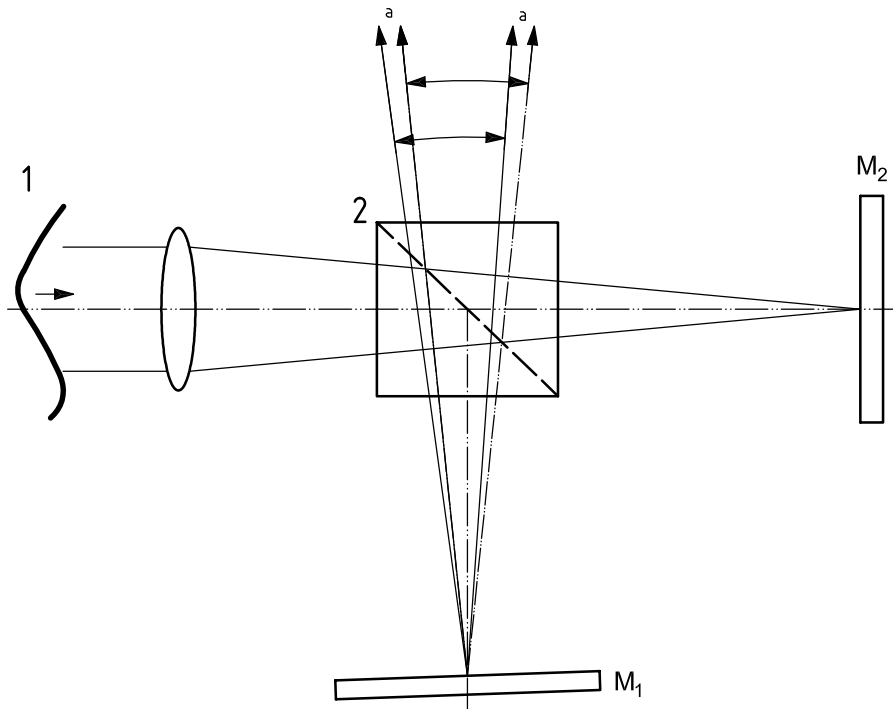
### 5.3.2.3 Shearing methods

Because there can be large deviations of a general aspheric wavefront from a simple wavefront like a plane or spherical wavefront, interferometric techniques that give a low number of fringes are desired. The method in most widespread use is shearing interferometry where a wave surface generated by the aspheric is compared with a duplicate of itself. This duplicate can be generated in different ways. It can be an identical but laterally shifted, rotated, or flipped duplicate. To extract all of the information, it is necessary in some cases to measure in two orthogonally independent shear dimensions. A typical example could be a Michelson interferometer where the aspherical wave is focused onto the mirrors which are tilted to provide a lateral shear of the two wavefronts (see Figure 8).

Other alternatives as the Ronchi grating and other compact two-beam interferometers are extensively described in the literature [5].

An alternative especially suitable for slow aspherical wavefronts is radial shear interferometry where a laterally magnified version of the aspheric wavefront is compared with the original wavefront (see Figure 9).

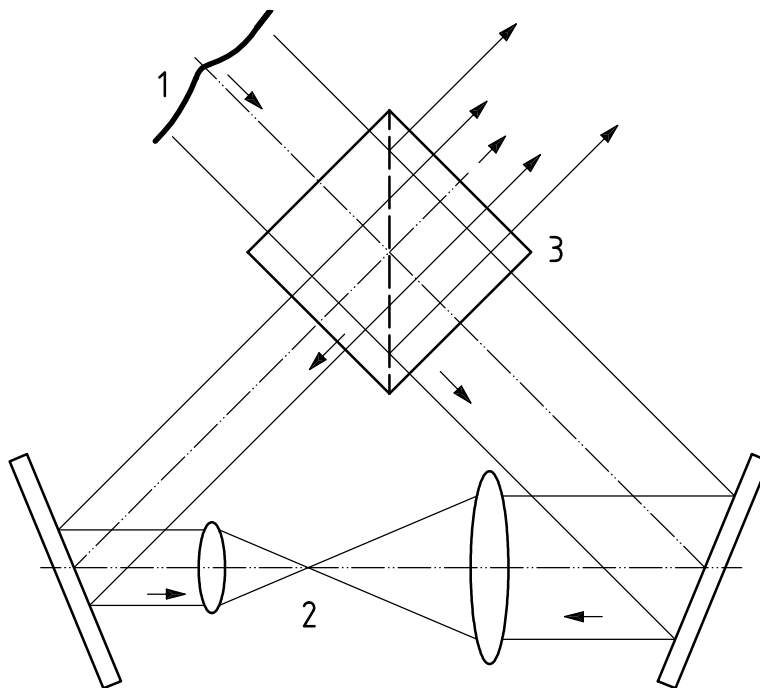
For slow aspheres, the radial shear can be made so big that in a first approximation the interferograms directly show the deviations in a nearly absolute manner.



**Key**

- 1 aspheric wavefront
- 2 beam splitter
- a To detector.
- $M_1$  Mirror 1
- $M_2$  Mirror 2

**Figure 8 — Shearing interferometer on the basis of a Michelson interferometer**



**Key**

- 1 aspheric wavefront
- 2 telescope
- 3 polarizing beam splitter

**Figure 9 — Cyclic shearing interferometer providing radial shear**

### 5.3.2.4 Null tests using refractive optics and computer-generated holograms

A successful interferometric test set-up keeps the wavefront deformations small at the beam-splitting devices to avoid systematic errors and awkward evaluation procedures.

This can be accomplished by using some compensating optics which generates a conjugate wavefront to the wavefront refracted or reflected by the aspheric lens/mirror. If the ideal asphere generates a wavefront having the complex amplitude  $e^{ikW_a(x,y)}$ , then the compensating optics (null lens) should generate the conjugate wavefront  $e^{-ikW_a(x,y)}$  so that in an appropriate series arrangement a nearly plane (besides the deviations of the real wavefront from the ideal) wavefront is produced which can interfere with a plane reference wave. At first sight this concept seems to be contradictory, since modelling  $e^{-ikW_a(x,y)}$  requires in general cases complicated optical systems which for themselves can not be tested with sufficient accuracy since they produce the same aspherical wavefront deformation only with opposite sign.

But if the null lens can be made with only a few (or even single) spherical lens components, which for themselves can be tested with spherical surface tests, then the null lens problem can be solved with sufficient reliability.

However, the preferred alternative is the use of diffractive optical elements or computer-generated holograms (CGH). Such holograms can represent any wave aberration. It is well known [6] that CGH commonly generate at least two first orders whose phase functions are phase conjugates of each other. So inevitably the illumination of such a CGH, e.g. with the plane reference wave, will produce at least two first diffraction orders in addition that can be separated by spatial filters.

There are three possibilities for inserting the CGH.

- a) The CGH is inserted into the parallel arm of the interferometer used for testing and directly replaces a real master.
- b) The CGH is used for compensating the aspheric wavefront to produce a plane, spherical, or otherwise known reference wave; it is therefore inserted into the same beam as the aspheric surface and replaces a null lens.
- c) The CGH is inserted after the interferometer and produces information about the aspheric surface in a Moiré pattern.

By using asymmetric phase reliefs, such holograms can be produced having mainly only one diffraction order. These holograms have been applied to aspheric testing [7], [8], [9] and are also known for the rotational symmetric case as kinoforms [10].

To reduce the computation and production problems to a reasonable level, it is necessary to make the distance between the null lens/CGH and the asphere as small as possible in order to avoid wavefront warping. The latter effect is well known from steep aspheres having no stigmatic properties. Steep aspheres are part of optical systems where they serve as a wavefront compensator. The Schmidt-plate is one typical example. The most advantageous CGH-null lens has a plane wavefront entering the combination of CGH and asphere. Figure 10 shows a transmitted light arrangement.

By using a blazed CGH, a configuration for reflected light (see Figure 11) can also be made.

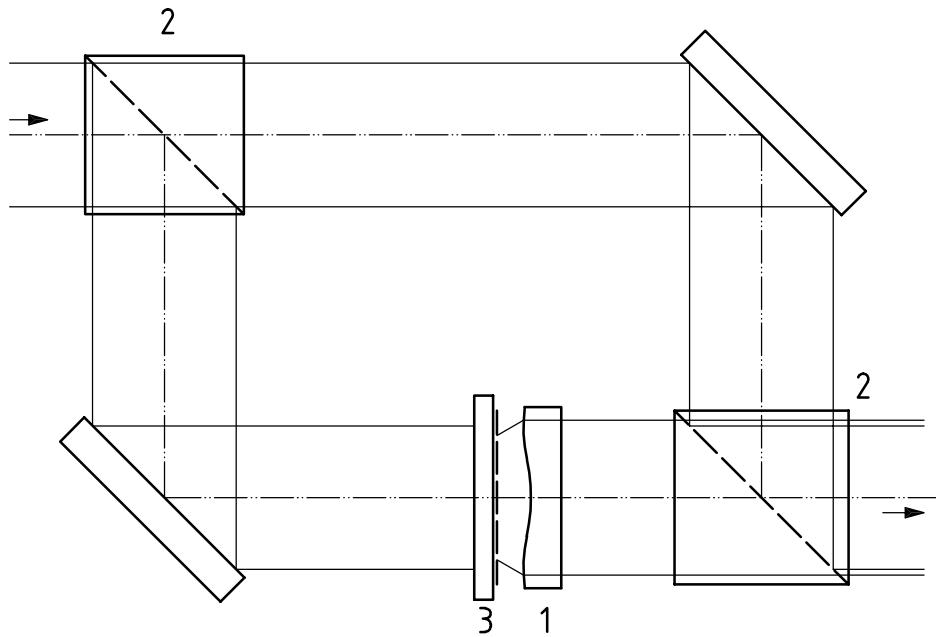
These configurations have a significant advantage that the interferometric components are traversed by approximately plane wavefronts which guarantees freedom from systematic measuring errors.

If strict symmetry is obeyed for the interferometric set-up, the other conjugate wavefront can also be employed by arranging the CGH in the reference arm (see Figure 12).

The CGH can also be positioned outside of the interferometer if the deviations of the asphere are not too severe and systematic errors stay within tolerable limits. The resulting test interferogram can be interpreted as a Moiré fringes between the CGH structure and the interference pattern in the CGH-plane, or if spatial filtering

is used, the diffracted reference wave and the zero order of the object wave are superimposed to give the deviations of the asphere from the ideal surface (see Figure 13).

Rotational symmetric aspheres can be tested with rotational symmetric CGH's. Since all diffraction orders are on axis, there will be a small disturbance of the interferogram in the centre. If the aspheric deviation is very small, so that a sufficient separation of different diffraction orders becomes difficult, one can add some quadratic phase function to represent a defocus term. The use of such rotational symmetric CGH (RSH: for rotational symmetric hologram) reduces the spatial frequency content of the CGH, considerably alleviating the printing process of the CGH (see Figure 14).

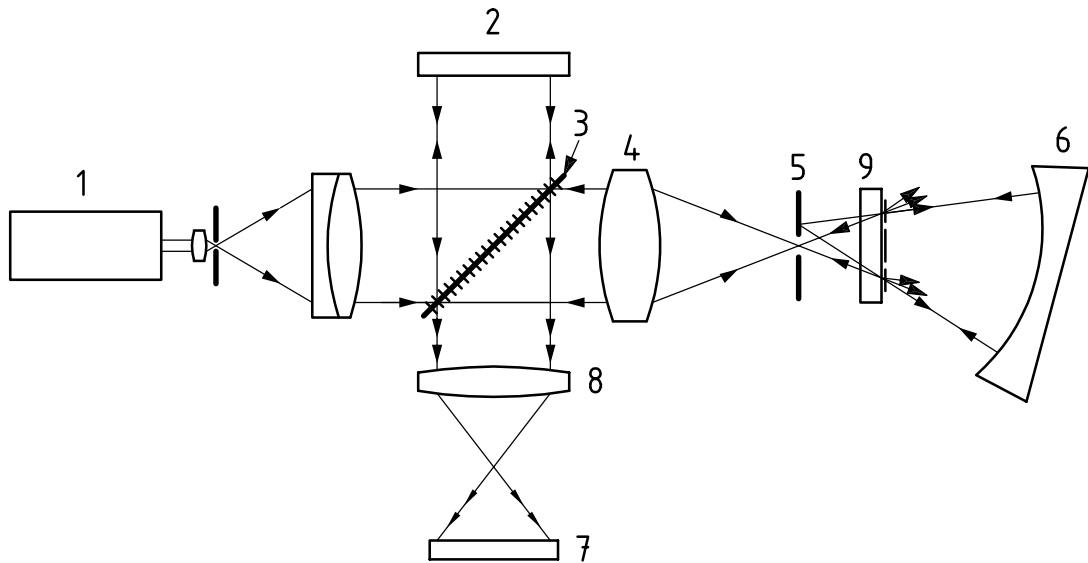


**Key**

- 1 aspherical lens
- 2 polarizing beam splitter
- 3 CGH

**Figure 10 — Computer-generated hologram (CGH) as null lens for a transmitted light test of an aspheric lens**

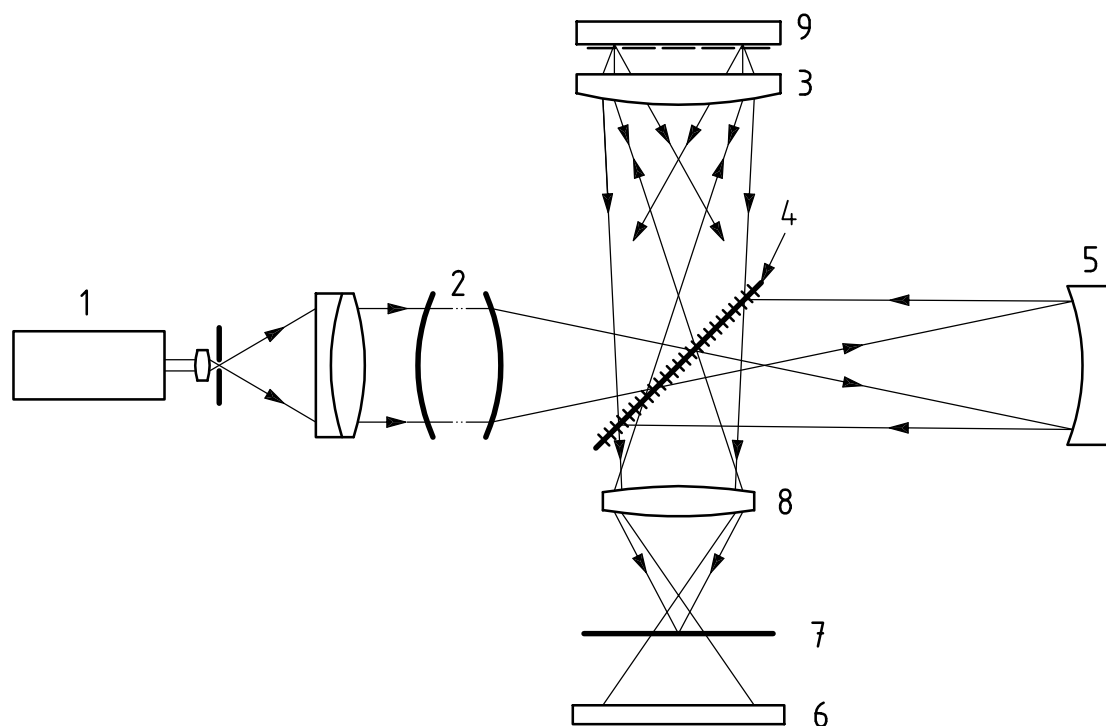


**Key**

- 1 laser
- 2 reference mirror
- 3 beam splitter
- 4 diverger
- 5 spatial filter
- 6 asphere
- 7 interference plane
- 8 imaging lens
- 9 CGH

A diverger with a CGH and the aspheric mirror in series are inserted into one arm of a Michelson interferometer. From the entering spherical wave the CGH generates a wave which meets the mirror everywhere at right angles. After reflection and further diffraction at the CGH, an approximately spherical wave is generated which carries the deviations of the aspheric surface.

**Figure 11 — CGH compensation of an aspheric surface**

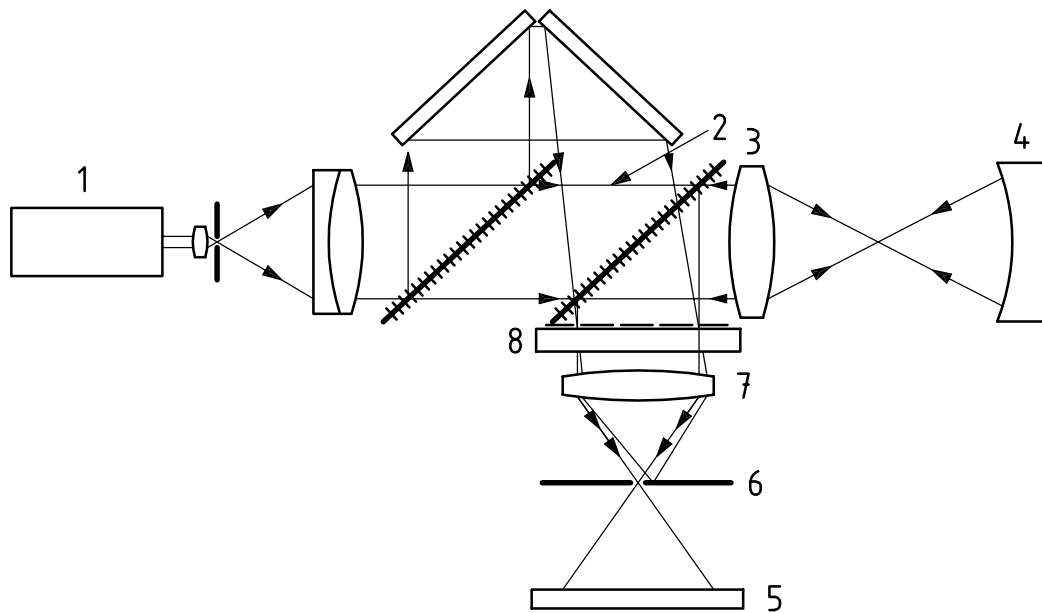


**Key**

- 1 laser
- 2 condenser
- 3 auxiliary lens
- 4 beam splitter
- 5 asphere
- 6 interference plane
- 7 stop
- 8 imaging lens
- 9 CGH

The auxiliary lens is used to produce the spherical curvature of the wavefront. The CGH only generates aspheric deviations.

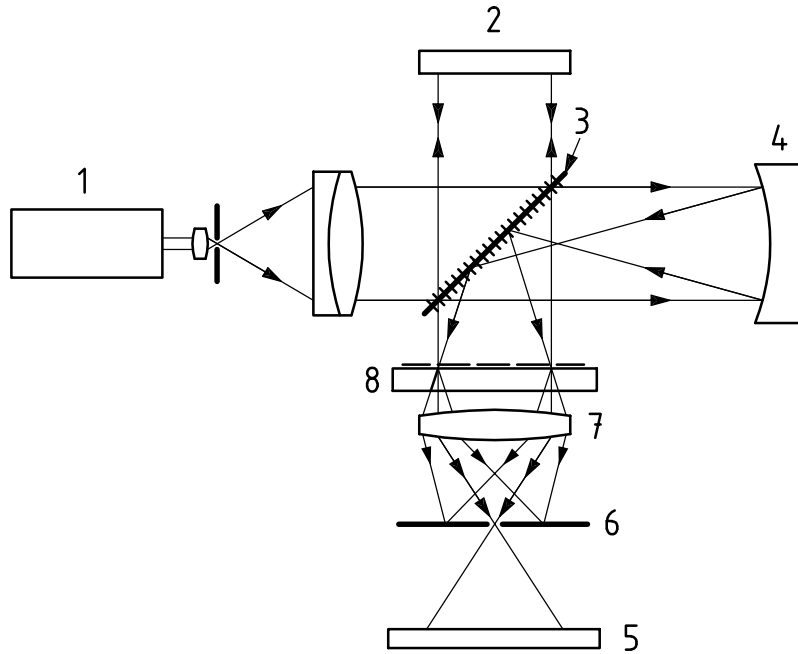
**Figure 12 — Michelson interferometer with a combination of auxiliary lens and CGH**

**Key**

- 1 laser
- 2 reference wave
- 3 diverger
- 4 mirror to be tested
- 5 interference plane
- 6 spatial filter
- 7 imaging lens
- 8 CGH

The CGH is illuminated by a plane wave and produces, in the first order of diffraction, a reference wave for the wave reflected at the aspheric mirror to be tested. A spatial filter separates the diffracted from the undiffracted light.

**Figure 13 — Interferometer in series arrangement with a carrier frequency CGH**



- Key**
- |                    |                                       |
|--------------------|---------------------------------------|
| 1 laser            | 5 interference plane                  |
| 2 reference mirror | 6 spatial filter                      |
| 3 beam splitter    | 7 imaging lens                        |
| 4 parabolic mirror | 8 rotational symmetric hologram (RSH) |

An entering plane wave is transformed at a parabolic mirror into a spherical wave. The latter is diffracted at the RSH and interferes with the plane reference wave, which is reflected into the same direction by the reference mirror.

**Figure 14 — RSH test for aspheric mirrors**

**5.3.2.5 Relative test of aspheres**

In holography one has the possibility of storing a wavefront on a photographic plate, if certain limitations regarding the spatial frequency apply<sup>[11]</sup>. When testing smooth surfaces, these conditions are generally fulfilled.

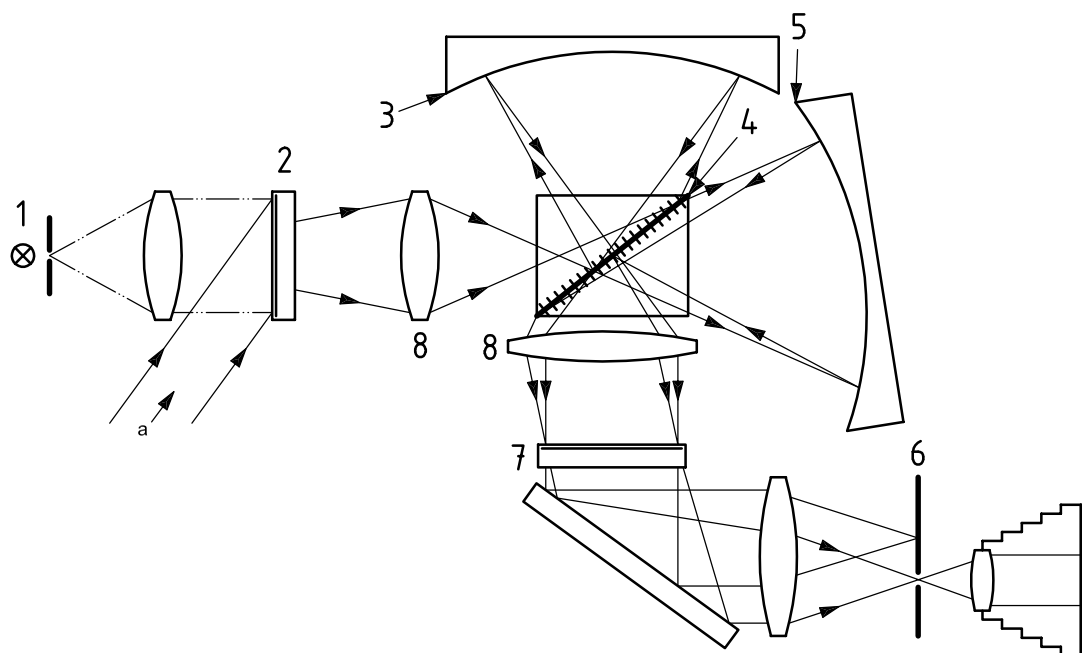
Thus one can, for instance, store a state in a hologram, which would not otherwise be available for comparison on account of changes which the object might undergo, e.g. correction of the surface or further polishing. Here real-time holography offers the possibility of comparing two states at time  $\tau_1$  and  $\tau_2$ . If high accuracy and reproducibility of the results are required, holographic methods will be problematic, if the carrier frequency in the hologram is too high. In this case, lateral shrinking of the photographic layer is particularly noticeable. Furthermore, the holographic plates are, in general, not sufficiently stable, and this also leads to disturbances of the wavefront.

In some cases, it is useful to reduce the carrier frequency by fitting the shape of the reference wave of the object. Such a method was described for spheres<sup>[12]</sup>. The method can also be applied to aspheric surfaces. For this purpose, two aspheric surfaces of similar shape are inserted into a Twyman-Green interferometer (see Figure 15). By fitting the shapes of the aspheric surfaces A and B (or C) to one another, a carrier frequency hologram of low frequency (here Hologram II) can be used for storing the deviations of the surface B from A. Since the interferometer is not perfect, the use of a difference method when comparing the aspheric surfaces B and C is necessary to compensate for errors. Since the surface A is used as a reference surface, its deviations when comparing the surface B to the surface C are also eliminated. To obtain the difference between the deviations of the surfaces C and B, the Moiré fringe comparison between Hologram II,

which has stored the deviation difference the surfaces A and B, and the live-fringe pattern of the surfaces A and C is used. Here the contrast is at first relatively small. To improve the contrast, it is necessary to block the wave of the zero diffraction order.

But with strongly deformed aspheric surfaces, a separation of the zero and first orders of diffraction is not possible if the carrier frequencies are small (e.g. 10/mm), since the position of strongest constriction of the beam extends further than the spacing between the zero and first orders of diffraction. To compress the cross-section of the beam, the wave entering the interferometer is deformed in advance in such a way that, after reflection at the aspheric surfaces A, B, or C, almost spherical waves are produced. These then pass through an almost point-shaped region. Hologram I serves to deform the wave in advance. This is obtained via phase conjugation by superposing an aspheric and a plane wave, which enter from the same side with respect to the hologram. For reconstruction, a plane wave enters from the back and in reverse direction. Reference [13] shows that in this case, even the deformation of a wave formed by a diffuser can be compensated.

Here an aspheric mirror takes the place of the latter, whose effect is cancelled in this way. Figure 16 shows the deviations of two aspheric surfaces from each other with parallel and wedge adjustment. The Twyman-Green arrangement and the pre-compensation of the wavefront furnish important aides for adjustment. On the one hand, white light interference fringes can be used for adjustment, on the other, observation of the focal plane of the pre-compensated wavefront makes it possible to supervise the pre-adjustment of the repositioned surfaces B or C (Figure 17). In this way, different aspheric surfaces of the same batch and different states of the same aspheric surface can be compared, and knowledge of the rotational symmetry of a surface can be attained.



#### Key

- |                      |  |
|----------------------|--|
| 1 white light source | 5 asphere B (or C)                     |
| 2 Hologram I         | 6 selection of first diffraction order |
| 3 asphere A          | 7 Hologram II                          |
| 4 beam splitter      | 8 imaging lens                         |
| a From laser.        |  |

The Hologram I serves to illuminate the interferometer. After reflection at the aspheric surfaces A, B or C, approximately spherical waves are reflected. The deviations of the surface B from A are stored in Hologram II. After replacing B by C, the deviations of the surface C from B can be measured. The white light source serves for the adjustment of the centres of the two aspheres relative to each other.

**Figure 15 — Doubly compensated hologram interferometer for testing aspheric surfaces**

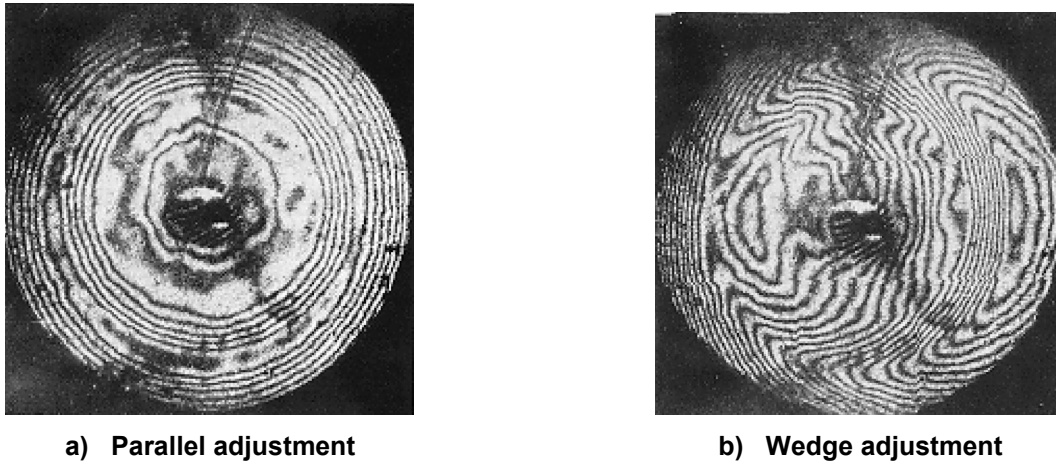


Figure 16 — Deviations of two aspheric surfaces from one another (distortions due to the interferometer are eliminated)

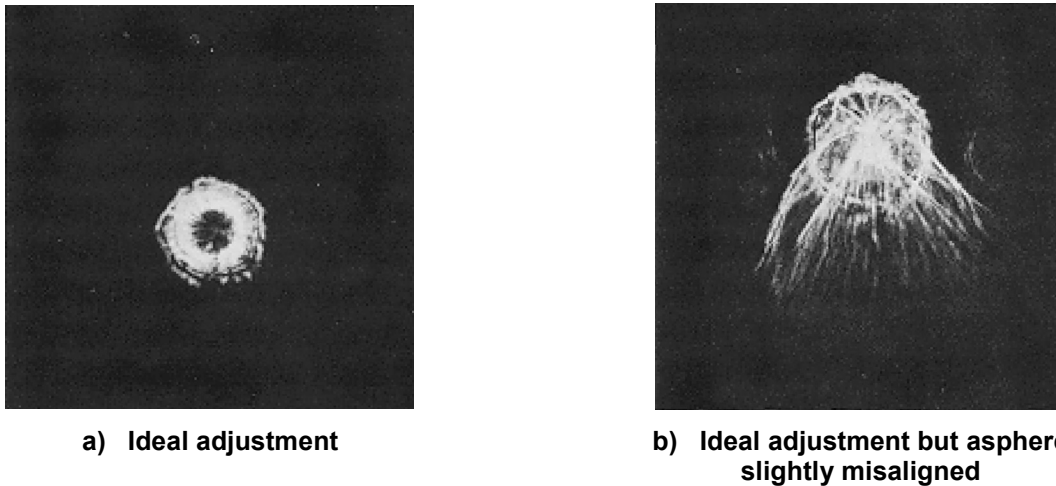


Figure 17 — Section through the light beam near to the plane of strongest beam constriction (slightly defocused)

## 5.4 Homogeneity testing

### 5.4.1 General

Testing the homogeneity of a sample requires the object to be transparent for the wavelength used in the Michelson interferometer. It also needs the object have at least two face-to-face polished surfaces. If they are not polished, then the user has to insert the sample in a cuvette and fill the free volume with an index-matching liquid.

In both cases, the user places the sample in the measurement arm of the Michelson interferometer and observes an interference pattern if the condition of sufficient source coherence is achievable. The adjustment is made by taking into account the competition between path difference compensation and apparent mirror translation due to the sample thickness.

The observed interference pattern is the result of the summation of three interference sources:

- first surface of the sample;
- homogeneity of the sample refractive index;
- second surface of the sample.

In order to extract the homogeneity information from the observed interference pattern, the user has to determine the different contributions.

#### 5.4.2 Faces contributions

The user has to determine the surface quality of both faces of the sample. He may use a variety of different techniques, in order to know how the two faces contribute to the observed interference pattern. Some possible techniques are indicated in 5.4.2.1 to 5.4.2.3.

It is very important that the technique used gives an accurate knowledge of the relative positions of surfaces and/or surface defects, because of the algebraic summation of the defects in the definitive result (face 1 + face 2 + internal homogeneity).

##### 5.4.2.1 Source coherence

By using a source of short coherence (for example a high-pressure discharge lamp or a white light source), the user is assured that his measurement of the contribution from the first surface of the sample is free from information coming from the second face of the sample.

##### 5.4.2.2 Coating the surfaces

If a reflecting coating is deposited on a surface to transform it into a mirror, the reflecting surface can be used as a mirror in the measurement arm of the interferometer, and its quality (flatness, defaults) can be measured.

##### 5.4.2.3 Tilting the sample

By tilting the sample a little bit, the user can then separate the beams returning from the two sample surfaces. The beam reflected on the first surface can then be arranged to interfere with the beam returning from the reference arm, by an equal tilting of the reference mirror, and the passing of returning beams through the mixing (beam-splitting) plate. The user thereby has access to the surface quality.

### 5.5 Optical systems in transmission

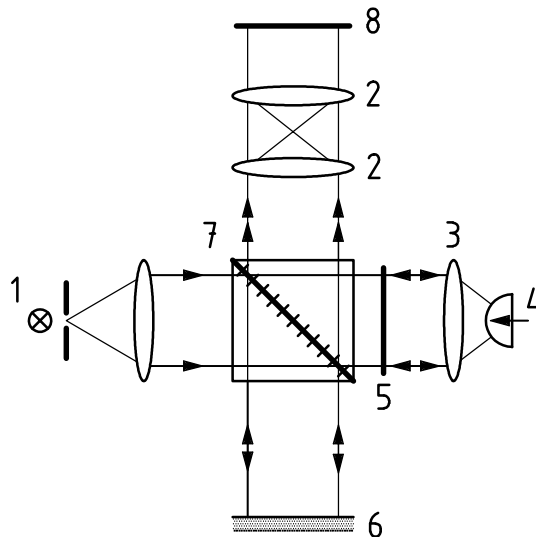
Optical systems can be measured in a Twyman-Green set-up (see Figure 18). This is for quality optical systems that have only moderate wave aberrations. This enables a double-pass geometry which is the basic arrangement after Twyman Green. Diffraction limited performance assumes calibration of the interferometer, since otherwise the limited accuracy of the optical components would obscure the wave aberrations to be measured.

The ideal optical system transforms spherical wavefronts of different curvature into one another. So it is understandable that calibration procedures rely on absolute planeness and sphericity tests for optical surfaces (see Clause 6).

For the calibration of an interferometer used in the test of optical systems, assume that a plane and a spherical surface of suitable curvature and diameter have been tested absolutely and the test data are stored in a computer memory [14].

With these elements and data, absolute values can be obtained for the wave aberrations of an optical system by using a two-step process provided the aberrations of the system are only small. Greater wave aberrations may cause different light paths through the lens system on the return path due to the double-pass

arrangement. So, in principle, the accuracy depends to some degree on the achieved correction of the system under test, which is very common in physical measurements and is one special case of the general conflict between measuring range and accuracy.



**Key**

- 1 light source
- 2 imaging optics
- 3 optical system under test
- 4 reference surface
- 5 planar wavefront
- 6 reference mirror
- 7 beam splitter
- 8 charged-coupled device (CCD)

**Figure 18 — Scheme of a Twyman-Green interferometer**

a) Step 1 The plane normal surface with the surface deviations  $P(x, y)$  is inserted in the Twyman-Green interferometer in front of the lens to be tested (Figure 18). Then one obtains a Michelson interferometer showing the following aberrations:

$$W_1(x, y) = W_{\text{ref}}(x, y) + 2P(x, y) \tag{8}$$

where  $W_{\text{ref}}(x, y)$  are the deviations of the interferometric components.

b) Step 2 The Twyman-Green interferometer is used in the normal test geometry with a known spherical normal surface having the deviations  $S(x, y)$  related to the coordinate system in the exit pupil of the optical system. The resulting wave aberrations are then:

$$W_2(x, y) = W_{\text{ref}}(x, y) + 2W_{\text{optsys}}(x, y) + 2S(x, y) \tag{9}$$

c) Step 3 From these two equations the aberrations of the optical system can be calculated:

$$W_{\text{optsys}}(x, y) = \frac{1}{2} \{ W_2(x, y) - W_1(x, y) - 2[S(x, y) - P(x, y)] \} \tag{10}$$

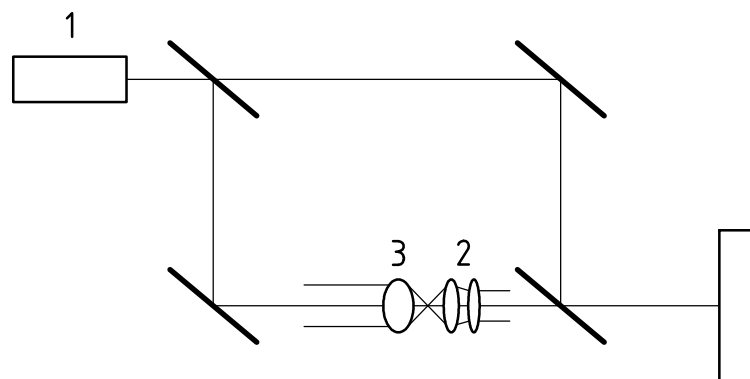


In order to bring all coordinate systems, i.e. those in the exit pupil of the optical system under test and the coordinate systems on the plane and the spherical surface, into coincidence careful calculations and scaling operations have to be carried out.

To ensure the accuracy in the coordinate transformations, fiduciarities can be used on the sphere and on the plane mirror.

Alternatively, interferometric lens tests would make whole-reference systems necessary. If again for the sake of simplicity, the  $\infty/f$  test-configuration is assumed, at least one beam converger/diverger is needed to correctly illuminate the system under test (see Figure 19). Furthermore, high-quality mirrors and beam splitters are needed if a Mach-Zehnder type interferometer is to be used. On first sight, the influence of the plane mirrors of the interferometer might be expected to be eliminated by storing the phase deviations of the empty interferometer first and then measuring the combination auxiliary system plus lens under test and finally subtracting the empty interferometer data set from the second one. However, the lens combination introduces an inversion in the test arm making the solution of a secure absolute test rather involved.

One solution could rely on three-system methods known from sphericity tests or methods using rotations and translations of the lens under test relative to the frame of the instrument [7]. [15].



#### Key

- 1 laser
- 2 objective to be tested
- 3 reference objective

**Figure 19 — Transmitted light test**

Only in the case of shearing methods (see Figure 20), the need for high-quality optics may be reduced to an additional diffraction-limited auxiliary system which in its turn could be calibrated by the just described procedure relying on absolutely tested flats and spheres. In the latter case, the wavefront can of course be measured in front and behind of the two systems combination and in this way get rid of all other influences onto the accuracy of the test.

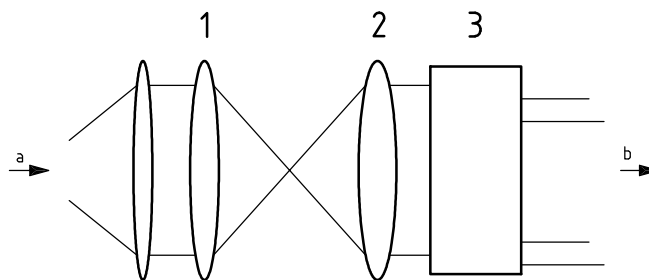
Absolute values for the wave aberrations and in this sense reliable secondary merit functions as point spread function (PSF) and modulation transfer function (MTF) within the framework of allowed approximations can only be obtained by using absolute test methods known from planeness and sphericity surface tests. This makes special adjustment facilities and complicated evaluations necessary, which should be reserved to national institutes.

However, interferometric tests may also be useful if the highest accuracy is not the main objective but a mere indication is required whether the optical system fulfils the design goals. In this case, special interferometric arrangements might be useful also. One such simple device is the Smartt-Interferometer [5] where an interferogram can be generated by letting the central part of the focused wavefront be diffracted at a very fine pinhole and allowing the remainder of the wavefront to pass the diffracting screen but with strongly reduced amplitude. The attenuation can be adjusted by choosing the transparency of the diffracting screen appropriately.

In this arrangement, an interferogram is obtained indicating aberrations and also the shift of focus introduced by movements of the pinhole in the caustic focus region of the optical system under test.

Other arrangements allow the determination of the even or the odd part of the wave aberrations. So, for example, a rotational shear between the interfering wavefronts through an angle of 180° provides the odd part of the wave aberrations. While a double-pass geometry with a cat's eye adjustment of an optical system in one arm of a Twyman-Green interferometer results in the even part of the wave aberrations provided the deviations of the interferometer components can be neglected [5].

Alternatively, radial shear instruments are also useful for the test of optical systems. The evaluation becomes rather simple if the system under test produces a strong beam compression in the test arm or if, in case of a cyclic interferometer, one beam is expanded and the anticyclic one is compressed by the same factor. The expanded beam will show only small aberrations compared to the compressed beam. In this sense, a suitable reference beam is obtained due to the scaling of the beam cross-sections.



**Key**

- 1 auxiliary optics
- 2 system under test
- 3 lateral shearing interferometer

- a From laser.
- b To detector.

**Figure 20 — Lateral shearing interferometer for measuring wave aberrations**

## 6 Optical test procedures for achieving absolute calibration

### 6.1 General

To attain high accuracy in interferometric optical testing, the effects of systematic interferometer errors, including the reference surface error, have to be removed in the final results. This can be accomplished by calibrating the interferometer with the help of a standard specimen, e.g. a standard surface. The known deviation data of the standard are used to correct the interferometer data in the memory of the on-line computer.

Basic standards in this context are flats and spherical surfaces. Methods for establishing flat and spherical standards are dealt with in 6.2 and 6.3, respectively. The deviation data of a standard have to be known as deviation from an ideal mathematical reference surface (flat or spherical, respectively). In this sense, these deviations are often called absolute deviations. The interferometric methods which are used to determine absolute deviations are called absolute interferometric methods. This term is to be seen in contrast to relative methods which have been dealt with in Clause 5.

In 6.2 and 6.3, the most important of these methods are taken into consideration. Absolute interferometric methods are described in detail in the strict sense as just defined, using a minimal number of positional combinations and proven to be successful in practice. Consequently, these methods are recommended. The choice of the method described depends on its purpose. For example, if a flat standard is used in a horizontal

position, the absolute method of 6.2.1 can be used. If, on the other hand, a flat standard is used in a vertical position, the methods of 6.2.2 or 6.2.3 are more suitable. Moreover, if a flat standard is to be manufactured to the highest possible level of surface precision, several manufacturing steps are necessary. Between these steps, absolute measurements are necessary but only to a comparatively low lateral resolution. Here, for example, the method of 6.2.3 is suitable. On the other hand, if the final measuring result (e.g. for certification) has to be obtained with a higher degree of lateral resolution, the methods of 6.2.2 should be used.

## 6.2 Flats

### 6.2.1 Liquid mirror [7]

An ideal plane can be created with the help of the law of gravity and its effect on the surface of a liquid. The following were recommended as suitable liquids:

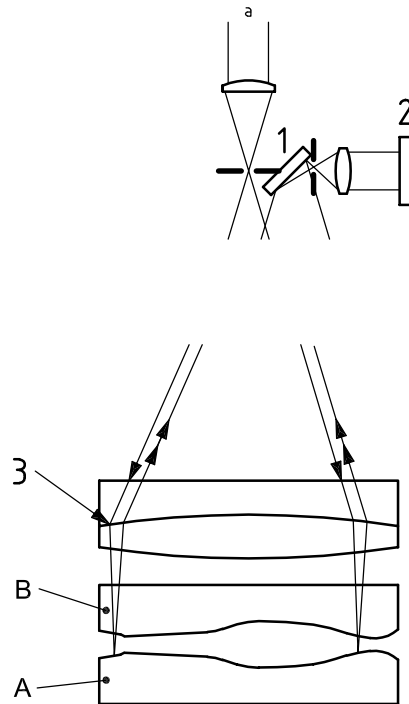
- medicinal liquid paraffin,
- water,
- mercury,
- silicone oil.

The optical arrangement consists of a Fizeau interferometer with horizontally placed surfaces; see Figure 21. In general, the lower surface (A) is the liquid mirror and the upper surface (B) the test surface. Under these conditions, it is necessary that the test sample be transparent, e.g. a glass plate. If, however, the test surface is opaque, it can be used as lower surface (A); however, it is necessary that the liquid immediately above, of course, then be transparent.

The choice of a suitable liquid is limited by the requirement that disturbing influences should be avoided. Some of the disturbing influences that have to be taken into account are

- mechanical vibration,
- temperature vibrations,
- evaporation effects,
- electric charges,
- capillary effects at the boundary,
- dust particles on the liquid,
- disturbances caused by unevenness of the bottom of the vessel when the layer of liquid is too thin,
- the effect of the curvature of the earth,
- sagging of the test surface by gravitation on account of the horizontal position required.

Sagging is a fault of general nature, which has been dealt with in ISO 14999-2:2005, 3.3.3. If the liquid mirrors are not too large, the effect of the earth's curvature is negligibly small; in any case this effect is known, and can be taken into account when necessary. The other effects entail certain requirements with regard to the properties of the liquid and the thickness of its layer. The reflectivity of the liquid mirror must be considered, as it affects the contrast and definition of the interference fringes. When using a mirror made of mercury, the test surface with its partially transparent aluminium coating is connected electrically with the mercury vessel, in order to allow charges formed during the cleaning of the test surface to drain away.



**Key**

- 1 mirror
- 2 detector
- 3 collimator

- A lower surface
- B upper surface

a From light source.

A, B: combination of the test surfaces.

**Figure 21 — Fizeau interferometer for testing optical flats**

**6.2.2 Three-flat rotation method [7]**

**6.2.2.1** The rotation method starts with three unknown optical flats, A, B, C. The flats are to be tested by interferometric comparison in a Fizeau interferometer. Figure 22 shows one of these flats. For an interferometric comparison, the flats are combined in pairs in different relative positions. Figure 23 shows such a combination. The rotation method uses four positional combinations of this kind for the absolute determination of the unknown flatness deviations. This determination is possible with a lateral resolution corresponding to an arbitrary number  $N$  diameters (central sections). Those four combinations are shown in Figure 24; they are the three usual basic combinations AB, BC, CA, and a fourth combination  $AB^\phi$ , in which flat B has been rotated by a certain angle  $\phi$  about the optical axis, as compared with its position in the basic combination AB. The angle of rotation  $\phi$  controls the lateral resolution and is determined by  $\phi = 360^\circ \times M/N$ . Here  $M$  and  $N$  are natural numbers that are prime to each other and  $N$  is the number of diameters that can be evaluated exactly so that  $2N$  points on any circle about the surface centre can be resolved. In Figures 23 and 24,  $M = 1$  and  $N = 10$ .

The resulting interference pattern can be evaluated in such a way that the unknown flatness deviations are determined. The following equations hold

for AB 
$$x_{\nu+}y_{-\nu} = D_{\nu} - d_{\nu} = a_{\nu} \tag{11}$$

according to Figure 22, and correspondingly:

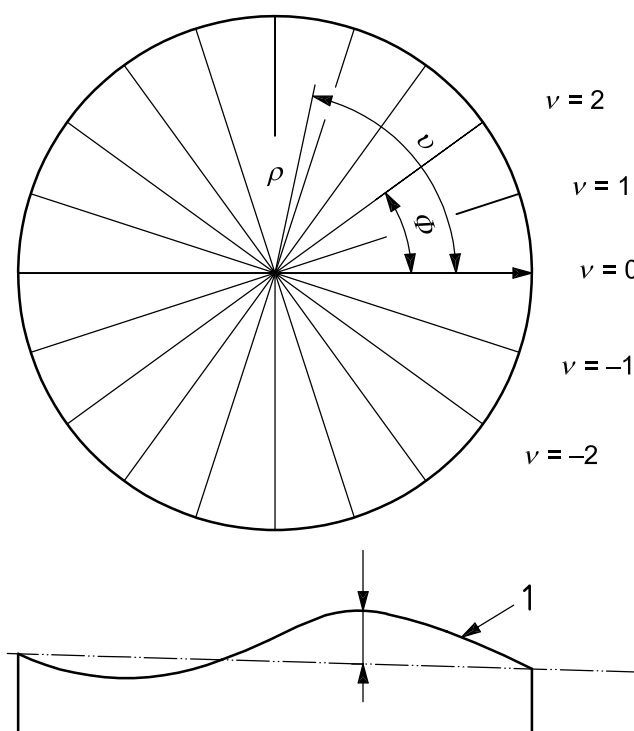
for BC  $y_\nu + z_{-\nu} = b_\nu$ , (12)

for CA  $z_\nu + x_{-\nu} = c_\nu$ , (13)

for AB<sup>φ</sup>  $x_\nu + y_{2-\nu} = a_\nu$ . (14)

Each of the four lines of equations stands for 2N equations with  $\nu = -N + 1, -N + 2, \dots, N$ .

These equations hold and can be separately solved for any constant  $\rho$  value, where  $x_\nu$  is the flatness deviation of A at the azimuth  $\nu = \nu\phi/2$  and, correspondingly,  $y_\nu$  the one of B, and  $z_\nu$  the one of C.  $D_\nu$  is the (in the beginning unknown) distance between the ideal reference planes.

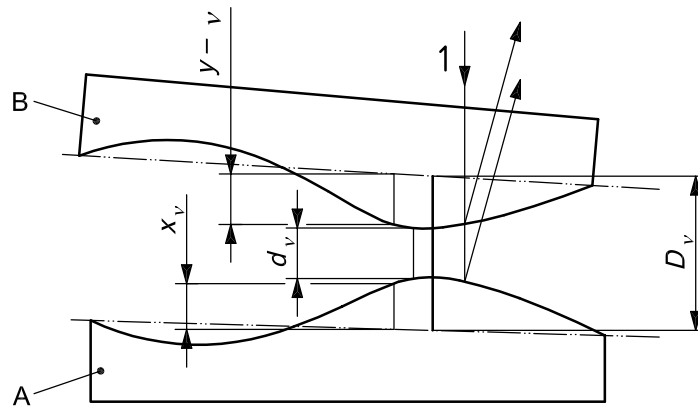


**Key**

1 optical surface to be tested

[The polar coordinate system ( $\rho, \nu$ ) is appropriate here. The unknown deviations of the optical surface from the reference plane (dashed line) are to be determined.]

**Figure 22 — One of the three flats (A, B, or C) in top view and side view**

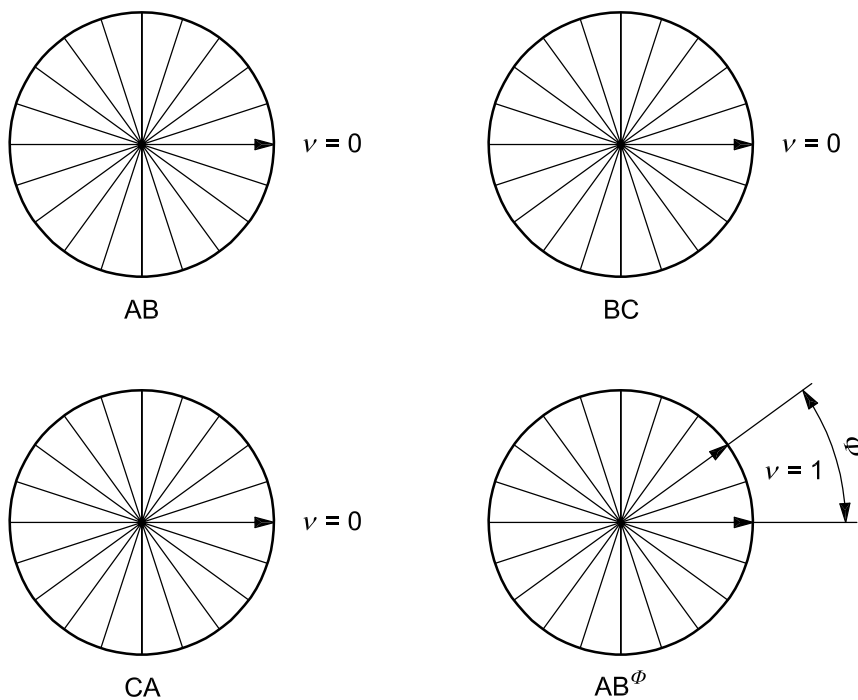


**Key**

1 light

The surface distance  $d_v$  is known by an interference measurement, i.e. it is known apart from an additive constant, which is not of interest. The distance between the reference planes is  $D_v$ . The unknown flatness deviations  $x_v$  and  $y_v$  are to be determined. Functions of the positions are  $d_v$ ,  $D_v$ ,  $x_v$  and  $y_v$ .

**Figure 23 — Combination AB in side view**



In the fourth combination,  $AB^\phi$ , Flat B has been rotated from its position in the first combination, AB, by an angle  $\phi$ . The coordinate systems of all three surfaces are oriented so that in the first three combinations, which are the basic combinations, the azimuths  $\nu = 0$  of both flats coincide (coincidence is at  $\nu = 0$ ). Then in the fourth combination, which is the rotational combination, the azimuths  $\nu = \phi/2$  coincide (coincidence is at  $\nu = 1$ ).

**Figure 24 — Four positional combinations in top view**

Least-squares methods for determining and minimizing the effect of random measuring errors permit optimal resolution in depth and an enhanced lateral resolution. The r.m.s. error of determining a flatness deviation can be calculated as a function of the r.m.s. measuring error, the desired lateral resolution, and the position on the surface.

In computer-aided interferometers usually square-grid area detector arrays are used. The centres of the individual detectors (or a part of them) can be taken as square-grid nodes, in which the distances between the unknown flats are directly known by measurement. The rotation method, on the other hand, proceeds from known distances between the flats at the nodes of a polar grid (coordinate system according to Figure 22; measured distance between the flats is  $d_v$  in Figure 23). The transition between the two grids or coordinate systems can be carried out by a local interpolation method.

**6.2.2.2** In summary, for the absolute testing of flats by the rotation method, the following main steps should be carried out.

- a) Three flats A, B, C are combined in pairs in four different positions according to Figure 24 in a Fizeau interferometer. In each of these four positional combinations, the distances between the surfaces at the measuring points are read and stored.
- b) From the stored surface distances, mean measuring errors can be calculated. If the measuring errors are too large, improved measurements should be made.
- c) In the case of a square or rectangular detector grid, the corresponding data in the polar grid are calculated by interpolation.
- d) From these data in the polar grid the absolute flatness deviations (e.g.  $x_v$  in Figure 23) are calculated (absolute determination).
- e) After step d), the absolute flatness deviations are available in the polar grid; now they can be interpolated back into the square or rectangular grid.
- f) The absolute flatness deviations available at the nodes of the grids can be further processed for surface parameters such as contour lines, three-dimensional plots, quality values, and others.

**6.2.2.3** To carry out step a) in 6.2.2.2, the following procedural conditions should be fulfilled.

- a) The plates to be tested should be mounted vertically, i.e. the surface normals should be horizontal. Then changes in sag of the plates during the testing do not have to be taken into account. Sag can cause systematic errors if the plates are used in another orientation after absolute testing. In such a case, when sag can occur, it has to be taken into account. This can be accomplished to some extent, e.g. by modelling the plate mathematically and calculating the sag to be expected.
- b) The two surfaces under test that are combined in the respective relative measurement have to be imaged onto the camera chip. Here the image of the coordinate system of one of these two surfaces and the coordinate system of the camera chip itself should coincide. The axes of the Cartesian coordinate system of the camera chip should have the directions of the pixel rows and columns and the centre of this coordinate system should be a preset pixel (i.e. a reference pixel), preferably near the geometrical centre of the chip.
- c) For the fourth combination ( $AB^\phi$  in Figure 24), the second of the two plates of the first basic combination has to be rotated by an angle  $\phi$ . This rotation has to be carried out about the surface normal at the surface coordinate origin.
- d) The diameter of the circular interferogram on the camera chip has to have at least a certain preset number of pixel distances. The phase values measured at the pixels within that circle are used to calculate the absolute flatness deviations.
- e) The plates to be tested absolutely have to be mechanically and thermally stable. Therefore, in addition to conditions a) to d) concerning geometrical relations between the plates and the interferometer, the plates

themselves have to fulfil certain geometrical relations concerning their dimensions. They have to be manufactured from proper material, they have to be held in a special mount so that deformations of the plates by mechanical stress from clamps or the dead weight are avoided, and they have to be installed in a sufficiently temperature-controlled environment.

As an example, Table 1 shows maximum allowable tolerances of the conditions a) to c) for the specific case of  $M = 7$ ,  $N = 30$ , i.e.  $\Phi = 84^\circ$ , a camera chip of  $256 \times 256$  pixels, a circular interferogram with a preset diameter of 232 pixels, and a systematic measuring error, caused by interferometer misalignment, of below  $\lambda/300$  for reasonable surfaces. The rotation angle of  $\Phi = 84^\circ$  makes possible a lateral resolution in the result that corresponds to a square grid of approximately  $30 \times 30$  points in the result. This means that, in the result, here 500 to 600 square-grid points of the surface are resolved independently.

For still higher lateral resolution at the same level of accuracy (resolution in depth) in the result, a fifth positional combination can be added. This is a second rotational combination in which flat B has been rotated by an angle of  $K\Phi$ ,  $\Phi$  being the rotation angle of the fourth positional combination of step a) of 6.2.2.2. With  $N$  being the wanted number of diameters,  $K$  should be chosen according to the relation  $K \approx \sqrt{N}$  ( $K$  the nearest integer). So, a lateral resolution of e.g.  $128 \times 128$  points in the result can be easily obtained.

**Table 1 — Maximum allowable tolerances**

Condition	Concern	Tolerance
1	Horizontal surface normals	$\pm 5^\circ$
2	Coincidence of the reference pixel and the images of the centres of the surface coordinate systems	$\pm 1$ pixel
	Coincidence of the reference pixel and the geometrical centre of the chip	$\pm 5$ pixels
3	Rotation angle $\Phi$	$\pm 0,1^\circ$
	Coincidence of the directions of the rotation axis and the surface normal	$\pm 1^\circ$
	Coincidence of the rotation axis with the reference pixel	$\pm 1$ pixel

**6.2.3 Three-flat Zernike method** [5], [20]

This method differs from the basic three-flat rotation method of 6.2.2 in the algorithm for determining the absolute deviations from the stored surface distances of step a) of 6.2.2.2. The procedural conditions themselves are nearly the same. So, four positional combinations according to Figure 24 are used, namely the three basic positions and one rotational position with an angle  $\Phi$  of rotation of flat B against flat A.

If, in analogy to the equations of 6.2.2, the test surface deviations are denoted by  $x(\xi_i, \eta_j)$ ,  $y(\xi_i, \eta_j)$ , and  $z(\xi_i, \eta_j)$ , and the measured test surface differences in the four positional combinations are denoted by  $a(\xi_i, \eta_j)$ ,  $b(\xi_i, \eta_j)$ ,  $c(\xi_i, \eta_j)$ , and  $a'(\xi_i, \eta_j)$ , with  $(\xi_i, \eta_j)$  being the coordinates of the measured points  $(i,j)$ , then each of the seven functions  $x(x_i, h_j)$  to  $a'(x_i, h_j)$  can be represented by a set of Zernike polynomials of the form.

$$\sum_{n,m} R_n^m(r) [U_n^m \cos(m\theta) + U_n^{-m} \sin(m\theta)] \tag{15}$$

Here,  $(r, \theta)$  are polar coordinates in the unit circle ( $\xi = r \cos \theta$ ,  $\eta = r \sin \theta$ ),  $R_n^m(r)$  are the radial polynomials, and  $U_n^m$ ,  $U_n^{-m}$  are coefficients associated with the even (cosine) and odd (sine) terms, respectively. The Zernike polynomial coefficients of the four measured functions  $a$  to  $a'$  have to be calculated, and from them the polynomial coefficients of the three functions  $x$ ,  $y$  and  $z$  can be obtained by linear equations. Then the figure of each of the flats is determined up to the order of the fit, i.e. the surface deviations are characterized by a set of independent numbers (coefficients) according to the order of the polynomials chosen. The number of these coefficients, usually of the order of 40 to 50, corresponds to a number of independently resolvable points of the same order of magnitude. That is, here 40 to 50 points of the surface can be resolved independently.



As an example of the determination of Zernike polynomial coefficients of the three surfaces, the determination of the surface focus coefficients  $l_4$ ,  $m_4$ , and  $k_4$  of  $x(\xi_i, \eta_j)$ ,  $y(\xi_i, \eta_j)$ , and  $z(\xi_i, \eta_j)$ , respectively, is given. These coefficients are determined from the following equations:

$$l_4 + k_4 = E_4 \quad (16)$$

$$m_4 + k_4 = G_4 \quad (17)$$

$$k_4 + l_4 = D_4 \quad (18)$$

$$l_4 + m_4 = F_4 \quad (19)$$

where  $E_4$ ,  $G_4$ ,  $D_4$  and  $F_4$  are the test wavefront focus coefficients of  $a(\xi_i, \eta_j)$ ,  $b(\xi_i, \eta_j)$ ,  $c(\xi_i, \eta_j)$  and  $a'(\xi_i, \eta_j)$ , respectively. The solution is:

$$m_4 = \frac{E_4 + F_4}{4} + \frac{G_4 - D_4}{2} \quad (20)$$

$$k_4 = G_4 - m_4 \quad (21)$$

$$l_4 = \frac{E_4 + F_4}{2} - m_4 \quad (22)$$

Structural similar equations hold for all Zernike coefficients.

## 6.3 Spherical surfaces

### 6.3.1 General

Strictly speaking, the interferometric methods used to determine absolute deviations of spherical surfaces as mentioned in 6.1, and dealt with in this subclause, are methods to determine sphericity. The mean radius of the spherical surface is not determined. The radius may be measured by other methods, a variety of them being well known but described elsewhere.

In general, this does not cause a problem because in a wide variety of applications, the accuracy by which the radius of a spherical surface has to be known is at least one order of magnitude below the accuracy which is required for deviations from sphericity.

In 6.3.2 and 6.3.3, two methods are described. The three-position method (6.3.2) is mathematically simple but well suited only for spherical surfaces having smaller radii of curvature. The rotation-shift method (6.3.3) needs a higher computational effort but is well suited for small as well as long radii up to the infinite and gives a very effectively working instrument for compensation of measuring errors.

### 6.3.2 Three-position method [1], [7]

This method can be used with both Fizeau and Twyman-Green interferometers. It determines the absolute deviation by measuring the even and odd parts of the deviation. It can be derived by making three interferogram evaluations. To demonstrate the principle, let us consider the Twyman-Green case. The following positions of the surface to be tested are used (Figure 25):

- a) basic position, surface illuminated perpendicularly, and the wavefront in the interferometer exit is:

$$W_a(\mu, \nu) = R(\mu, \nu) + O(\mu, \nu) + N(\mu, \nu) \quad (23)$$

- b) turned position, surface illuminated perpendicularly but rotated through 180° about the optical axis, and the wavefront in the interferometer exit is:

$$W_b(\mu, \nu) = R(\mu, \nu) + O(\mu, \nu) + N(-\mu, -\nu) \quad (24)$$

- c) cat's eye position, surface vertex coinciding with focus, and the wavefront in the interferometer exit is:

$$W_c(\mu, \nu) = R(\mu, \nu) + \frac{O(\mu, \nu) + O(-\mu, -\nu)}{2} \quad (25)$$

$R$ ,  $O$ , and  $N$  represent the wave aberrations caused by the reference arm of the interferometer, the beam-shaping optics, and the surface to be tested, respectively.  $(\mu, \nu)$  are rectangular coordinates on the surfaces. The solution of the equations for  $N(\mu, \nu)$  is

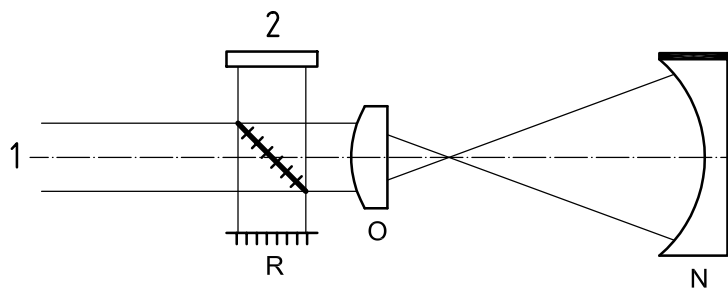
$$N(\mu, \nu) = \frac{W_a(\mu, \nu) + W_b(-\mu, -\nu)}{2} - \frac{W_c(\mu, \nu) + W_c(-\mu, -\nu)}{2} \quad (26)$$

The deviation of the surface itself results from this equation by multiplication with (1/2).

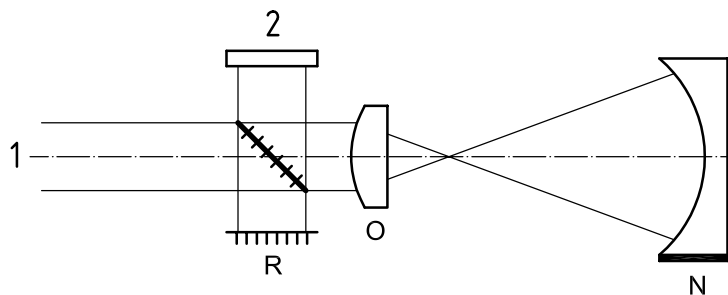
This method yields the absolute deviations in points determined by sampling points of the detector.

### 6.3.3 Rotation-shift method [15]

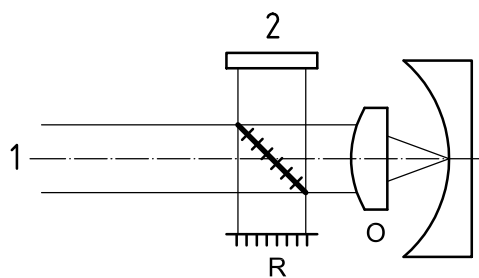
The method starts with relative comparisons which can be carried out, e.g. in a spherical Fizeau interferometer or in a Twyman-Green interferometer. Figure 26 shows a spherical Fizeau interferometer (the following relates to this example). A and B are two unknown sphericity standards or master surfaces to be tested (A is convex, B concave). For their illumination, a micro-objective can be used. The light reflected at A interferes with the light reflected at B. The resulting interferogram represents a relative comparison of the two unknown surfaces A and B. At least three of such interferograms are taken. In each of them, B is in a different lateral or rotational position with respect to A. Figure 27 shows four such positions (seen in light direction). Three positions are necessary for the method, the fourth is useful for increasing the accuracy. In each of these positions, the centres of curvature of A and B nearly coincide.



a) Position a



b) Position b

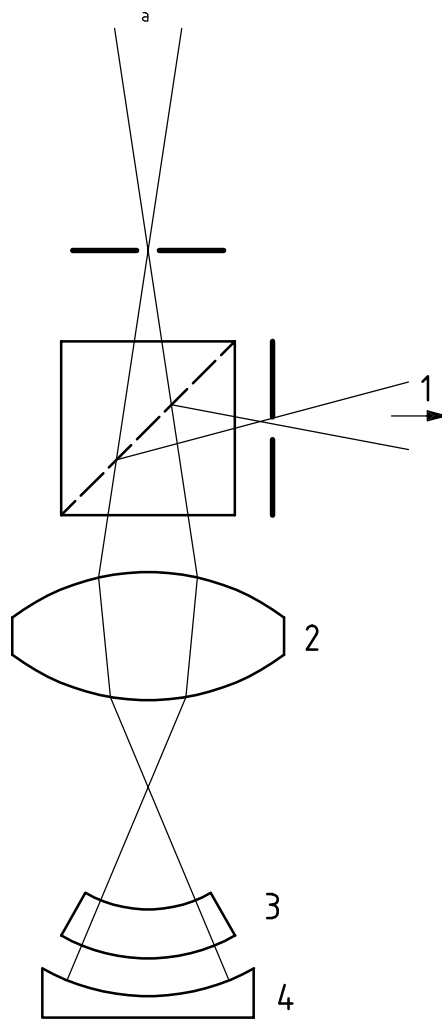


c) Position c

**Key**

- 1 laser
- 2 camera
  
- R reference
- O beam-shaping optics
- N surface to be tested

**Figure 25 — Three-position method**



**Key**

- 1 detector
- 2 micro-objective
- 3 master A
- 4 master B

a From laser.

**Figure 26 — Set-up for the rotation-shift method**

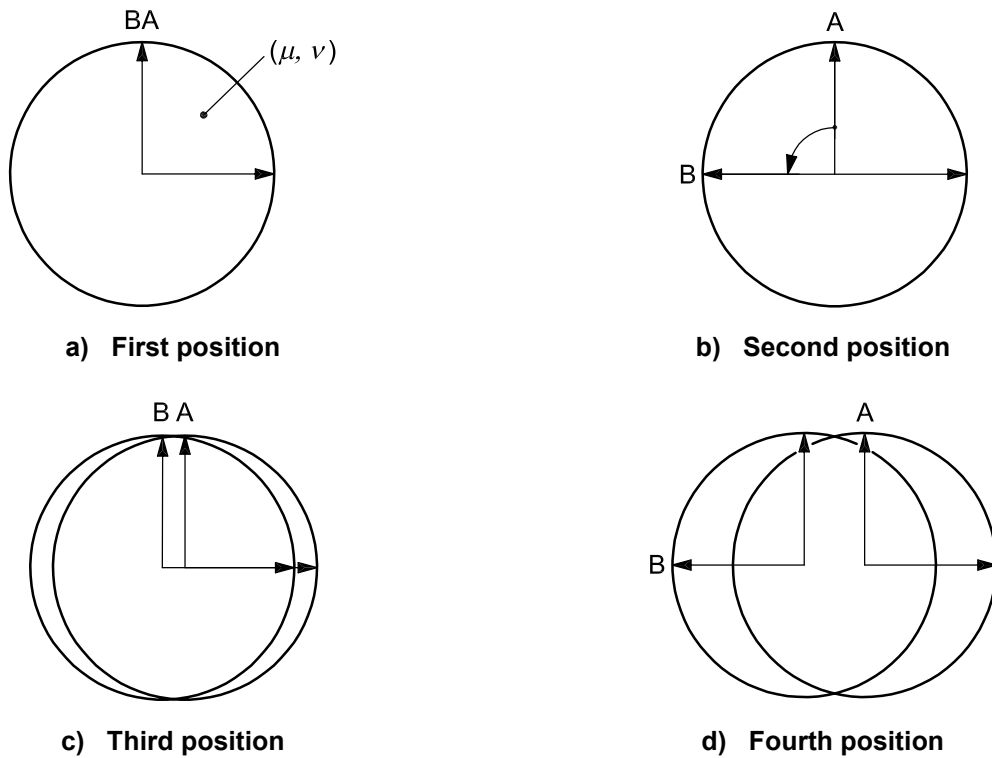


Figure 27 — Positions of the rotation-shift method

The four resulting interferograms are measured and computationally evaluated and combined in a suitable way. One way, which is restricted to small ratios of the diameter of the surfaces to be tested to their radius of curvature of, say, less than 1:4, is described in the following.

This yields the required surface deviations of A and B from two ideal reference spheres fitted in the least-squares sense. This is achieved by proceeding with the following equations, which hold in points  $(\mu, \nu)$  of a quadratic pattern in the respective positions:

a) First position:

$$x_{\mu\nu} + y_{\mu\nu} + A_0 + \mu A_1 + \nu A_2 + (\mu^2 + \nu^2)A_3 = a_{\mu\nu} \quad (27)$$

b) Second position:

$$x_{\mu\nu} + y_{\nu, -\mu} + B_0 + \mu B_1 + \nu B_2 + (\mu^2 + \nu^2)B_3 = b_{\mu\nu} \quad (28)$$

c) Third position:

$$x_{\mu\nu} + y_{\mu+1, \nu} + C_0 + \mu C_1 + \nu C_2 + (\mu^2 + \nu^2)C_3 = c_{\mu\nu} \quad (29)$$

d) Fourth position:

$$x_{\mu\nu} + y_{\nu, -\mu-3} + D_0 + \mu D_1 + \nu D_2 + (\mu^2 + \nu^2)D_3 = d_{\mu\nu} \quad (30)$$

e) A-sphere (all 4 positions):

$$\sum x_{\mu\nu} = \sum \mu x_{\mu\nu} = \sum \nu x_{\mu\nu} = \sum (\mu^2 + \nu^2)x_{\mu\nu} = 0 \quad (31)$$

f) B-sphere (all 4 positions):

$$\sum y_{\mu\nu} = \sum \mu y_{\mu\nu} = \sum \nu y_{\mu\nu} = \sum (\mu^2 + \nu^2)y_{\mu\nu} = 0 \quad (32)$$

The quantities  $x_{\mu\nu}$  are the unknown and required deviations of A from its reference sphere,  $y_{\mu\nu}$  are the corresponding deviations of B. The  $4 \times 4$  quantities  $A_0, \dots, D_3$  are unknown adjusting parameters. The quantities  $a_{\mu\nu}, b_{\mu\nu}, c_{\mu\nu}$  and  $d_{\mu\nu}$  are the negative spacings between the two surfaces A and B. The equations express the geometric spacing relations.  $\mu$  and  $\nu$  assume all permitted values. The equations of the last two lines fix the two ideal reference spheres concerning axial displacement, tilt, and curvature. The summations extend over the points  $(\mu, \nu)$ . The total number of equations amounts to, e.g., 292 if the required deviations  $x_{\mu\nu}$  and  $y_{\mu\nu}$  are to be determined at 81 points  $(\mu, \nu)$  of either surface. In this case, the total number of unknowns amounts to  $2 \times 81$  surface deviations +  $(4 \times 4)$  adjusting parameters = 178 unknowns. This system of linear equations needs to be solved.

For this the quantities  $a_{\mu\nu}, \dots, d_{\mu\nu}$  of the right sides of the equations need to be known. They are approximately known by the interferometric measurements, but they are not free from measuring errors. These measuring errors are now to be compensated. This is achieved by taking advantage of the fact that the number of Equation (27) to Equation (32) is greater than the number of unknowns. So the quantities  $a_{\mu\nu}, \dots, d_{\mu\nu}$  on the right of the equation should fulfil certain linear conditions identically, which can be expressed as follows:

$$\sum \alpha_{\mu\nu}^{(1)} a_{\mu\nu} + \sum \beta_{\mu\nu}^{(1)} b_{\mu\nu} + \sum \gamma_{\mu\nu}^{(1)} c_{\mu\nu} + \sum \delta_{\mu\nu}^{(1)} d_{\mu\nu} = 0$$

- 
- 
- 

(33)

$$\sum \alpha_{\mu\nu}^{(L)} a_{\mu\nu} + \sum \beta_{\mu\nu}^{(L)} b_{\mu\nu} + \sum \gamma_{\mu\nu}^{(L)} c_{\mu\nu} + \sum \delta_{\mu\nu}^{(L)} d_{\mu\nu} = 0$$

There are  $L$  equations (in the foregoing example  $L = 114$ ). Their coefficients  $\alpha_{\mu\nu}^{(1)}, \dots$  have been determined from the coefficients by the computer. The quantities  $\overline{a_{\mu\nu}}, \dots$  are the true or, at least, the most probable surface separations, and are not yet known, whereas the quantities  $-a_{\mu\nu}, \dots$  are their *measured* values and are already known. Now the quantities  $a_{\mu\nu}, \dots$  are determined by the following postulate. They have to approximate the measured values, in the least-squares sense, as closely as possible but on condition of fulfilling the equations. This means the postulate:

$$\sum (\overline{-a_{\mu\nu}} - a_{\mu\nu})^2 + \sum (\overline{b_{\mu\nu}} - b_{\mu\nu})^2 + \sum (\overline{c_{\mu\nu}} - c_{\mu\nu})^2 + \sum (\overline{d_{\mu\nu}} - d_{\mu\nu})^2 = \min \quad (34)$$

( $\overline{a_{\mu\nu}}, \dots, \overline{d_{\mu\nu}}$  being constant,  $a_{\mu\nu}, \dots, d_{\mu\nu}$  to be varied on the foregoing conditions)

In this way the measuring errors ( $\overline{a_{\mu\nu}} - a_{\mu\nu}$ ), ... are compensated.

The method may be developed further by introducing more than four positional combinations, by introducing rotations by angles other than right-angled and more different shifts, and by conquest the restriction to small apertures by introducing a more complex co-ordinate system, e.g. a system of spherical triangles.

## 6.4 Cylindrical surfaces

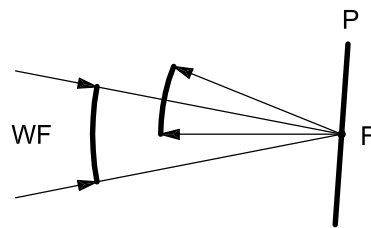
### 6.4.1 General

The principles of an absolute testing method of cylindricity in its strict sense without any material reference surface have been known for cylindrical surfaces since the seventies [7]. According to this method, three unknown cylindrical surfaces are compared interferometrically in pairs.

Other methods use flat or spherical surfaces as material references. The flat and spherical surfaces are tested beforehand by well-known absolute methods [9], [10] and are therefore absolutely known. Errors in absolute flatness and sphericity testing can usually be neglected as compared with permissible errors in testing cylindrical surfaces. These methods combine arithmetically the results of several specifically chosen relative measurements. In the individual relative measurements, the test specimen has specifically chosen positions compared with the interferometric test beam.

### 6.4.2 Tilting mirror method for cylindricity testing [16]

Figure 28 shows the principle of the tilting mirror method. The cylindrical wavefront WF, affected with unknown interferometer errors, meets, instead of an unknown surface to be tested, a known plane mirror P at the focal line F. WF is reflected at several specified angles in succession. By combining these measurements, the interferometer errors can be calculated. This way, the interferometer is calibrated. At least two angles of reflection are required.



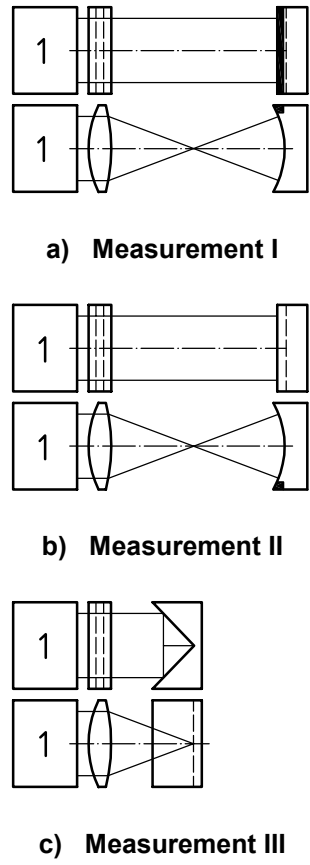
#### Key

- F focal line
- P plane mirror
- WF wave front

Figure 28 — Tilting mirror method

### 6.4.3 Roof mirror method for cylindricity testing [17]

Figure 29 shows the principle of the roof mirror method. Three measurements are used. In measurements I and II, a cylindrical specimen holds the normal position for relative testing in the test arm of the cylinder interferometer. Between I and II, the specimen is rotated by 180° around the optical axis. In measurement III, the specimen is replaced by a 90° roof mirror. The roof edge, the focal line of the cylindrical test beam, and the optical axis cross each other at right angles. By combining these measurements, the interferometer errors and at the same time the absolute surface errors of the test specimen can be calculated. Therefore, the interferometer is calibrated and the test specimen is now a standard.



**Key**  
 1 Twyman-Green interferometer

**Figure 29 — Roof mirror method**

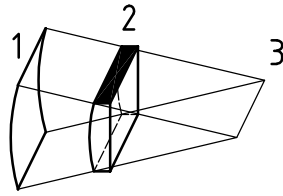
**6.4.4 Method for testing cylinders with long radii [18]**

Figure 30 shows the principle of the long radii method. At least four measurements are required. A fifth measurement can be added to increase the accuracy. The relative deviations of the cylindrical specimen are measured in three measurements, with the specimen in the second measurement b) being rotated around the axis of the cylinder by a small angular amount relative to the first and by 180° relative to the first measurement, in the third measurement c). The axis of rotation in the third measurement coincides with the optical axis of the interferometer. In the fourth measurement d), the relative deviations of the specimen are measured, with the specimen being displaced along the axis of the cylinder. In a fifth measurement, e), the absolute deviations of a section of the incident wave front of the test beam path can be measured along a straight line parallel to the axis of the cylinder, taking into account the known absolute deviations from straightness of a plane mirror placed in the beam path. For this purpose, the mirror should reflect the beams of the corresponding section itself.

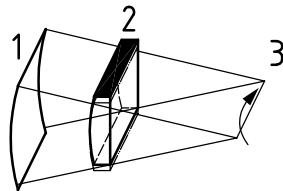
**6.5 Windows in transmission**

Absolute measurement of the wave aberration of an optical window can be performed by computing the difference of an empty interferometer and the same including the window under test. Back-reflection can be avoided by slight tilt.

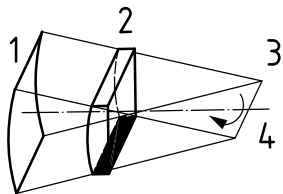




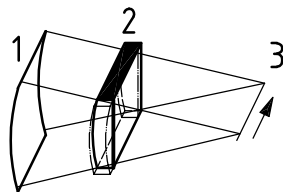
a) Measurement I



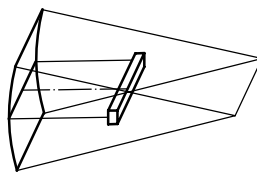
b) Measurement II



c) Measurement III



d) Measurement IV



e) Measurement V (optional)

**Key**

- 1 cylindrical testing wavefront
- 2 cylindrical surface to be tested
- 3 focal line
- 4 axis of rotation

**Figure 30 — Testing cylinders with long radii**

## Bibliography

- [1] JENSEN, A.E. Absolute calibration method for laser Twyman-Green wave-front testing interferometers. *J. Opt. Soc. Am.*, **63**, 1973, p. 1313
- [2] EVANS, C.J., and KESTNER, R.N. Test optics error removal. *Appl. Optics*, **35**, 1995, p. 7
- [3] FREIMANN, R., DÖRBAND, B., and HÖLLER, F. Absolute measurement of non-comatic aspheric surface errors, *Opt. Comm.*, **161**, 1999, pp. 106-114
- [4] DÖRBAND, B. Evaluation of rotational symmetric surface deviations by means of average radial profile, *Proc. SPIE*, **3739**, 1999, pp. 474-479
- [5] MALACARA, D. (ed.). *Optical shop testing*, John Wiley and Sons, New York, 1991
- [6] GOODMAN, J.W. *Introduction to Fourier Optics*, McGraw Hill, New York, 1968
- [7] SCHULZ, G., and SCHWIDER, J. Interferometric testing of smooth surfaces. *Progr. in Optics*, **13**, pp. 92-167, E. Wolf (ed.), North-Holland, Amsterdam, 1976
- [8] CREATH, K., and WYANT, J.C. Use of computer generated holograms in optical testing. *Handbook of Optics*, Vol. II, ch.13, McGraw Hill, New York, 1995
- [9] LOOMIS, J.S. Computer-generated Holography and Optical Testing. *Opt. Eng.*, **19**, 1980, pp. 679-685
- [10] LESEM, L.B., HIRSCH, P.M., and JORDAN, J.A. *IBM J. Res. Develop.*, **13**, 1969, p. 150
- [11] LEITH, E.N. and UPATNIEKS, J. Recent Advances in Holography. *Progr. in Optics*, **6**, pp. 1-52, E. Wolf (ed.), North-Holland, Amsterdam, 1967
- [12] SCHWIDER, J. and BUROW, R. Holographic comparison of smooth surfaces. *Proc. of the 2. Internationale Tagung Laser und ihre Anwendungen*, K 88, Dresden, 1973
- [13] LEITH, E.N. and UPATNIEKS, J. *J. Opt. Soc. Am.*, **56**, 1966, p. 523
- [14] SCHWIDER, J. Characterisation of interconnection components, pp. 109-148, in *Perspectives for parallel optical interconnects*, Lalanne and Chavel (eds.), Springer, Berlin, 1991
- [15] ELSSNER, K.-E., GRZANNA, J. and SCHULZ, G. Interferentielle Absolutprüfung von Sphäritätsnormalen. *Opt. Acta*, **27**, 1980, pp. 563-580
- [16] SCHULZ, G., BLÜMEL, T., KAFKA, R., ELSSNER, K.-E., VOGEL, A. Calibration of an interferometer for testing cylindrical surfaces. *Opt. Comm.*, **117**, 1995, pp. 512-520
- [17] BLÜMEL, T., ELSSNER, K.-E., KAFKA, R., SCHULZ, G., VOGEL, A. Absolute interferometric testing of cylindrical surfaces. *Proc. SPIE*, **2340**, 1994, pp. 250-257
- [18] ELSSNER, K.-E., BLÜMEL, T., BUROW, R., KAFKA, R., SCHULZ, G., VOGEL, A. *Proc. Int. Symposium on Laser in Precision Measurements*, Balatonfüred, Hungary, Akademie Verlag Berlin, 1996, p. 74-81
- [19] BRIERS, J.D. Interferometric optical testing: An interlaboratory comparison. *J. Opt. A: Pure Appl. Opt.*, **1**, 1999, pp. 1-14
- [20] FRITZ, B.S. Absolute calibration of an optical flat, *Opt. Eng.*, **23**, 1984, pp. 379-383
- [21] *Guide to the expression of uncertainty in measurement (GUM)*, BIPM, IEC, IFCC, ISO, IUPAC, IUPAP, OIML, 1993, corrected and reprinted in 1995

1

.....

---

---

**ICS 37.020**

Price based on 44 pages